Characteristics and sources of NMVOCs and the O_3-NO_x-NMVOCs relationships in Zhengzhou, China

Dong Zhang[1,3], Xiao Li[2,3], Minghao Yuan[4], Yifei Xu[4], Qixiang Xu[2,3], Fangcheng Su[2,3], Shenbo Wang[2,3], Ruiqin Zhang[2,3,*]

1 College of Chemistry, Zhengzhou University, Zhengzhou 450001, China

2 School of Ecology and Environment, Zhengzhou University, Zhengzhou, 450001, China

3 Institute of Environmental Sciences, Zhengzhou University, Zhengzhou 450001, China

4 Environmental Protection Monitoring Center Station of Zhengzhou, Zhengzhou 450007, China

Correspondence: Ruiqin Zhang (rqzhang@zzu.edu.cn)

Abstract:

Nonmethane volatile organic compounds (NMVOCs) are important precursors of ozone (O_3) formation under conditions of sufficient nitrogen oxides. Understanding the characteristics, emission sources of NMVOCs, as well as the relationship between NMVOCs and O_3 are of great significance for O_3 pollution control. In this study, a continuous online monitoring of NMVOCs from the 1st to the 30th of June was carried out in Zhengzhou, Henan Province. Furthermore, the study provided recommendations for strategies aimed at reducing O_3 formation. During the observation period, the concentration of total NMVOCs (TNMVOCs) varied from 9.9 to 60.3 ppbv, with an average of 22.8 ± 8.3 ppbv. The average concentration of TNMVOCs during O_3 pollution events was higher than that on the clean days. Six major sources of NMVOCs were identified by using the Positive Matrix Factorization model. Vehicular exhaust (28%), solvent usage (27%), and industrial production (22%) were the main sources. We explore observations of the O_3-precursors relationship and propose observation-oriented O_3 control strategies. The results of relative incremental reactivity (RIR) and empirical kinetics modeling approach showed that Zhengzhou was in the anthropogenic VOCs (AVOCs)-limited regime. NMVOCs had the largest RIR value, while NO_x exhibited a negative RIR value. It is noteworthy that the sensitivity of O_3 formation to biogenic VOCs was greater than that of AVOCs. Considering the reduction effect, it is recommended that the ratio of AVOCs to NO_x should be maintained at no less than 3:1 to effectively reduce O_3 formation.

Keywords: Emission reduction strategies; Positive Matrix Factorization; Relative incremental reactivity; The observation-based model; Empirical kinetics modeling approach

1 Introduction

In recent years, ozone (O_3) pollution has become increasingly prominent in China, especially in urban areas (Liu et al., 2023a; Zhao et al., 2021; Yan et al., 2023; Sicard et al., 2020). O_3 pollution has become an important factor affecting the ambient air quality (Zhang et al., 2023). Nonmethane volatile organic compounds (NMVOCs), as an important precursor of O_3 and secondary organic aerosols, widely exist in the atmospheric environment and participate in many photochemical reactions, which have an important impact on atmospheric oxidation capacity and air quality (Zhu et al., 2021). Some NMVOCs are also air toxics (Billionnet et al., 2011), such as benzene, trichloroethylene, and chloroform (Lerner et al., 2012). Long-term exposure to higher concentrations of NMVOCs can lead to acute or chronic risks (He et al., 2015). Therefore, it is necessary to continue to carry out NMVOCs monitoring activities in O_3 pollution areas to analyze NMVOCs concentrations levels, sources, and effects on O_3 generation.

The concentration of NMVOCs is affected by background concentration, weather conditions (Mo et al., 2015), emission sources, terrain conditions (Liu et al., 2016), and extent of pollutant transport (Shao et al., 2009). In addition, under meteorological conditions with higher temperature, NMVOCs exhibit photochemical losses during dispersion and regional transport (Zou et al., 2023; Liu et al., 2023a; Liu et al., 2020). As a result, the ambient NMVOC concentrations vary with the locality and season. For example, in typical coastal areas of Ningbo, the seasonal variation of NMVOCs concentrations were winter > spring > Autumn > summer (Huang et al., 2023). The coastal areas of Shandong Province had the highest value in winter (28.5 ± 15.1 ppbv) and the lowest value in autumn (14.5 ± 7.6 ppbv) (Huang et al., 2023). The average summer TNMVOCs concentration in the suburbs of Jinan (12.0 ± 5.1 ppbv) (Liu et al., 2023c) was lower than that in the suburbs of Beijing (18.3±8.9 ppb), and much lower than that in the central city of Beijing (44.0 ± 28.9 ppbv) (Wu et al., 2023). The average TNMVOCs concentration (21.7 ppbv) in the O_3 pollution period in Tianjin is 12% higher than that in the non-O_3 pollution period (Liu et al., 2023a).

NMVOCs are emitted from various sources including anthropogenic sources and biogenic sources (Chameides et al., 1992) as well as secondary generation through photochemical reactions (Yuan et al., 2012). The main sources of NMVOCs include motor vehicle emissions, industrial processes, solvent usage, fuel evaporation, combustion, and biogenic emissions (Wu et al., 2016; Prendez et al., 2013; Watson et al., 2001). Biogenic emission is mainly affected by temperature and radiation conditions (Li et al., 2020). Biogenic emissions are therefore higher during hotter months, especially in summer (Pacifico et al., 2009; Xu et al., 2023). Urban areas are greatly affected by anthropogenic sources (Zhang et al., 2023; Goldstein and Galbally, 2007). In different regions, the main contribution sources of NMVOCs are different. For example, the main

anthropogenic VOCs (AVOCs) sources in the Yangtze River Delta region of China are vehicle and solvent evaporation (Xu et al., 2023). The Pearl River Delta region is mainly affected by solvent use, liquefied petroleum gas use, and vehicle exhaust. Atmospheric NMVOCs in Beijing are greatly affected by motor vehicle emission sources and combustion sources (Liu et al., 2021; Zhang et al., 2020). Huang et al. (2023) reported that plastic synthesis, industrial processes, organic solvents, dyeing, traffic emissions, and pesticides were identified as the main sources of NMVOCs in Ningbo City in the coastal area (Liu et al., 2023b). Since different emission sources have different contributions to NMVOCs and thus have different impacts on the generation of O_3 (Zhang et al., 2023), it is necessary to investigate the sources of NMVOCs in different cities. Designing a reasonable and effective precursor emission control strategy is crucial to control the photochemical generation of O_3 (Yang et al., 2021). The relationship between O_3 and precursors is nonlinear (Chameides et al., 1992), and precursor emission reduction strategies need to be dynamically adjusted based on the actual sensitivity of O_3 formation (Chu et al., 2023; Lin et al., 2005). The observation-based model (OBM) is a widely used tool to analyze O_3-NO_x- NMVOCs sensitivity (Zhang et al., 2008; Nelson et al., 2021; Cardelino and Chameides, 1995). Several studies in China have analyzed the sensitivity of O_3 to precursors and control scenarios. For example, O_3 in the central area of the Yangtze River Delta is in a NMVOCs -limited regime, and AVOCs play a leading role in the formation of O_3 (Liu et al., 2023b). Chengdu is in a typical NMVOCs restricted area, so NMVOCs emission reduction helps to prevent and control O_3 pollution, and the emission reduction scenario based on NMVOCs source showed that the emission reduction ratio of NMVOCs to NO_2 needs to reach more than 3 to achieve prevention of O_3 pollution (Chen et al., 2022b). Xie et al. (2021) found that controlling NMVOCs in Leshan, a non-provincial capital city in southwest China, can effectively reduce the photochemical generation of O_3, and pointed out that the best emission reduction strategy for NMVOCs and NO_x should be 3:1. In addition, the generation of O_3 in areas such as Shanghai (Lu et al., 2023), Rizhao (Zhang et al., 2023), and Nanjing (Mozaffar et al., 2021) is generally limited by NMVOCs. However, in the United States and European countries, O_3 formation gradually transitioned from NMVOCs-limited regime to NO_x-limited regime (Nopmongcol et al., 2012; Ring et al., 2018; Goldberg et al., 2016).

Zhengzhou is the capital city of Henan Province and an important transportation hub in China. High population density levels, large vehicle ownership (MPS, 2022) and complex industrial structures determine the complexity of NMVOCs emission sources. In recent years, O_3 pollution in Zhengzhou has intensified, rendering it one of the cities with the highest O_3 pollution levels in central China (Wang et al., 2023b; Min et al., 2022). From 2020 to 2022, the annual 90th percentile of the mean daily maximum 8 h average O_3 (O_3-8H-90%) published by Zhengzhou Ecological Environment Bureau were 182, 177 and 178 μg/m^3, respectively,

which were 10% to 13% higher than the National Ambient Air Quality Grade II Standard (160 μg/m^3) (https://sthjj.zhengzhou.gov.cn/, last access: June, 2023). Some studies have analyzed the concentration levels, sources, and impact of NMVOCs on O_3 in Zhengzhou (Zeng et al., 2023; Wang et al., 2023b; Min et al., 2022). Wang et al. (2022) analyzed the sensitivity of O_3 to precursors and found that in July with low O_3 levels in Zhengzhou, O_3 formation was in a NMVOCs-limited regime, while on O_3 pollution accumulation and persistence days, O_3 formation was in a transitional state. Yu et al. (2021) showed that Zhengzhou was under a NMVOCs-sensitive regime in September. The above studies all show that it is important to study the emission reduction of precursors to control O_3 generation. However, there is still a lack of relevant research on June, the month with the highest O_3 pollution in Zhengzhou. In order to effectively solve the increasingly serious trend of O_3 pollution in Zhengzhou, it is necessary to give priority to and strengthen the research of Zhengzhou area, especially during the period of high O_3 pollution. Therefore, it is necessary to continue to pay attention to the pollution levels of O_3 and precursors in Zhengzhou and further explore the relationship between them.

In this study, we conducted an online measurement of NMVOCs in June, when O_3 pollution was severe in Zhengzhou. The concentrations, composition, and diurnal variation of NMVOCs in the atmosphere were analyzed. The main sources of NMVOCs were discussed by using ratio method and Positive Matrix Factorization (PMF) model. OBM was used to analyze the sensitivity of O_3-NMVOCs-NO_x and consequently the emission reduction strategy of precursors to control O_3 concentration was proposed. This study establishes a collaborative control strategy for atmospheric NMVOCs, which is of great significance for the control of atmospheric O_3 pollution in Zhengzhou.

2. Materials and methods

2.1 Sampling site

The monitoring site is on the roof (about 20 m above ground) of the building at Zhengzhou Environmental Protection Monitoring Centre Station (34.75° N, 113.60° E) (Fig. S1). The sampling site is a typical urban site, surrounded by residential areas, commercial areas, and office buildings. There are no point sources of air pollution nearby within a radius of 1 kilometer. The sampling site may be affected by motor vehicle and plant emissions.

2.2 Sample collection and chemical analysis

The sampling campaign was conducted from 1st to 30th June 2023. NMVOCs concentrations were observed with a gas chromatography-mass spectrometer, GC-MS (TH-PKU 300B, Wuhan Tianhong Instrument, China), which adopted detection technology of ultralow-temperature preconcentration combined with GC-MS/ flame

ionization detector (FID). The time resolution of the instrument is 1 hour, and the flow rate is 60 mL/min. The air sample was collected for the first 5 minutes of each hour and then pre-concentrated through a cold trap to remove H_2O_2 and CO_2. The sample was captured using an empty capillary column. After pre-concentration, the sample was desorbed by rapid heating and introduced into an analytical system. After separation by chromatographic column, the sample was detected by FID (for C2-C5 hydrocarbons) and MS (for C5-C12 hydrocarbons, halocarbons and OVOCs). The correlation coefficient of the standard curve of the target compound was greater than or equal to 0.99, and the detection limit of the instrument method was less than or equal to 0.1 nmol/mol. A total of 115 NMVOCs were monitored, including 29 alkanes, 11 alkenes, 1 alkyne, 17 aromatic hydrocarbons, 35 halogenated hydrocarbons, 21 OVOCs and 1 sulfide (carbon disulfide). Details of the device can be found in our previous study (Zhang et al., 2021). The individual NMVOCs concentrations measured during the observation period is shown in Table S1. Also the study conducted the simultaneous online measurements of hourly concentrations of particulate matter ($PM_{2.5}$ and PM_{10}), other trace gases (CO, O_3, NO, and SO_2), and meteorological data (temperature (T), relative humidity (RH), atmospheric pressure, and wind speed (WS) and wind direction (WD).

2.3 PMF model

The PMF 5.0 is an advanced multivariate factor analysis tool (USEPA, 2014), which can be used to identify the sources of NMVOCs (Norris et al., 2014). PMF model is expressed as follows:

$$X_{ij}=\sum_{k=1}^{p} g_{ik} f_{kj}+e_{ij} \quad (1)$$

where, i, j, and k represent the i^{th} sample, the j^{th} chemical species, and the k^{th} factor, respectively; X represents the chemical species concentrations measured in the sample; g is the species contribution; f is the species fraction; and e is the residual matrix.

The number of factors is obtained by minimizing objective residual function Q: as follows:

$$Q=\sum_{i=1}^{n}\sum_{j=1}^{m}\left[\frac{X_{ij}-\sum_{k=1}^{p} g_{ik} f_{kj}}{u_{ij}}\right]^2 \quad (2)$$

Where μ^{ij} is the sample data uncertainty.

The sample data uncertainty is calculated by Equations (3) and (4). If the data concentration is less than method detection limit (MDL), Equation (3) is used. Otherwise, Equation (4) is used.

$$Unc=\frac{5}{6}\times MDL \quad (3)$$

$$\mathrm{Unc}=\sqrt{(Error\ Fraction \times concentration)^2 + (0.5 \times MDL)^2} \quad (4)$$

where Error Fraction represent the precision (%) of each species;

Species with high proportions of missing samples or concentration values more than 25% below MDLs were excluded, while NMVOCs serving as typical tracers of emission sources were included (USEPA, 2014), and NMVOCs with short atmospheric lifetimes were excluded (Callén et al., 2014; Guo et al., 2011). In this study, 29 out of 115 NMVOCs collected over the sampling period was analyzed by the PMF model. In this study, a seven-factor solution ($Q_{true}/Q_{theoretical}$ = 3.42; and Fpeak = 0) was chosen (Fig. S2).

2.4 Conditional probability function analysis

The conditional probability function (CPF) is a source identification tool, which can be used to identify local emission sources of pollutants (Uria-Tellaetxe and Carslaw, 2014). CPF analysis methods were employed to determine the potential direction of emission sources by utilizing the wind directions and source contributions calculated through PMF (Kim and Hopke, 2004). The CPF is defined as:

$$\mathrm{CPF} = \frac{m_{\Delta\Theta}}{n_{\Delta\Theta}} \quad (5)$$

the variable $m_{\Delta\theta}$ represents the frequency of occurrences from the wind sector $\Delta\theta$ for the top 75% contributions of each identified NMVOCs source, while $n_{\Delta\theta}$ represents the total occurrences from the same wind sector. CPF analysis were constructed using the 'openair' package (Carslaw and Ropkins, 2012) in the statistical software R (R Foundation for Statistical Computing, Vienna, Austria).

2.5 OBM

OBM based on the Master Chemical Mechanism (MCM v3.3.1; https://mcm.york.ac.uk/MCM/) was employed to estimate the effect of changes in precursors on O_3 (Liu et al., 2022). Detailed information about OBM can be viewed in previous studies (Chu et al., 2023; Ling et al., 2011). Briefly, OBM is a zero-dimensional model that assumes a well-mixed atmosphere, and combined with atmospheric chemical mechanisms, simulates the O_3 production rate and the corresponding O_3 concentration at a given time (Kleinman, 2000).

The OBM used in this study iteratively solves a set of ordinary differential equations (ODEs) that describe the evolution of species concentrations over time. For species with observation concentrations (normally constituted by primary NMVOCs and NO_x), the horizontal convection and emission are normally significant. In a zero-dimensional model, those processes are lumped into R_{other} term. Within each iteration, R_{other} is determined by the Eq (6):

$$R_{other} = \left(\frac{\partial C_i}{\partial t}\right)_{obs} - \left[P_i - L_i C_i - \frac{1}{H} v_d C_i - \frac{1}{H}\frac{dH}{dt}\left(C_i - C_{i,bg}\right) + R_{aero,i} + R_{aq,i}\right] \quad (6)$$

Where P_i and $L_i C_i$ represents total the represents all the production and loss rate, respectively; $\frac{1}{H} v_d C_i$ represents the sum of mixing and deposition rates; $\frac{1}{H}\frac{dH}{dt}\left(C_i\text{-}C_{i,bg}\right)$ accounts for the mass exchange rate with background atmosphere; $R_{aero,i}$ and $R_{aq,i}$ are the rate of aerosol and aqueous processes, respectively; $\left(\frac{\partial C_i}{\partial t}\right)_{obs}$ is the real rate of change in concentration which is interpolated from hourly observed data points.

With the value of R_{other} term explicitly determined from Eq (6), the concentrations of all species are then predicted by integrating the governing equation (7):

$$\frac{\partial C_i}{\partial t} = P_i - L_i C_i - \frac{1}{H} v_d C_i - \frac{1}{H}\frac{dH}{dt}\left(C_i - C_{i,bg}\right) + R_{aero,i} + R_{aq,i} + R_{other} \quad (7)$$

New iterations start with updated R_{other} values based on the concentrations predicted from the previous step, until converged solution is obtained.

In this model, the net production rate O_3 ($P(O_3)$) is the difference between the O_3 production (the oxidation of NO by HO_2 and RO_2) and O_3 destruction (O_3 photolysis, reactions of O_3 with OH and HO_2, reactions of OH with NO_2, and reactions of O_3 with alkenes). This method for estimating O_3 production and removal rates has been utilized in several previous studies (Wang et al., 2017; Wang et al., 2022). The constants (k) represent the rate coefficients of the respective reactions, as follows:

$$P(O_3) = k_{HO_2+NO}[HO_2][NO] + \sum k_{RO_{2i}+NO}[RO_{2i}][NO] - k_{HO_2+O_3}[HO_2][O_3] - k_{OH+O_3}[OH][O_3] - k_{O(^1D)+H_2O}[O(^1D)][H_2O] - k_{OH+NO_2}[OH][NO_2] - k_{alkenes+O_3}[alkenes][O_3] \quad (8)$$

The relative incremental reactivity (RIR) was computed through OBM to evaluate the sensitivity of the photochemical production of O_3 to changes in the concentration of individual precursors within a given region (Ling et al., 2013; Cardelino and Chameides, 2000), which can be calculated from Eq. (9):

$$RIR(X) = \frac{[P_{O_3}(X) - P_{O_3}(X - \Delta X)]/P_{O_3}(X)}{\Delta S(X)/S(X)} \quad (9)$$

where X is the specific precursor of O_3; $P_{O_3}(X)$ and $P_{O_3}(X - \Delta X)$ are the net production of O_3 simulated by the OBM; and $\Delta S(X)/S(X)$ is the change in the concentration of S(X). The large change in primary pollutants (>20%) deviates greatly from the base scenario and is not representative of the current situation. Therefore, the concentration changes of $\Delta S(X)/S(X)$ were assumed to be 20%. In this study, the S for NMVOCs and NO_x were reduced by 0-100%. The relative change of $P_{O_3}(X)$ with S(NMVOCs) and S(NO_x) can be expressed by the isogram of $P_{O_3}(X)$.

The concentrations of trace gases (SO_2, O_3, CO, and NO), and meteorological parameters (T, RH, and WS) with 1 h time resolution were used as constraints in this model. At the same time, the concentrations of 75

NMVOCs observed with 1 h time were selected for input into the model because these 75 NMVOCs were included in MCM v3.3.1. The photolysis frequency ($J(H_2O_2)$, $J(NO_2)$) and planetary boundary layer are the default values. The setup and parameters of the OBM model are summarized in Table S2.

To evaluate the performance of this model, the index of agreement (IOA) was used in this study (Huang et al., 2005):

$$IOA = 1 - \frac{\sum_{i=1}^{n} (O_i - M_i)^2}{\sum_{i=1}^{n} (|O_i - \bar{O}| + |M_i - \bar{O}|)^2} \quad (10)$$

where O_i, M_i, and $\bar{O}$ represent the hourly values of observation, the simulation, and the average of observations, respectively. In various studies, model simulation results are often considered acceptable when the value of IOA falls within the range of 0.68 to 0.89 (Wang et al., 2018). To evaluate the reliability of our model simulations, we conducted an analysis of O_3 concentration in the atmosphere and calculated the IOA value. Our model does not directly incorporate O_3 observations. Instead, it utilizes concentrations of trace gases (SO_2, CO, and NO) and 75 NMVOCs, and meteorological parameters (T, RH, and WS) to simulate the concentration of O_3 in the atmospheric environment. The IOA values for O_3 was calculated from 7:00 to 19:00 during the day and obtained a result of 0.8. Therefore, the results simulated by our model are reliable.

3 Results and discussions

3.1 General characteristics

3.1.1 NMVOCs concentrations and composition

According to the national ambient air quality standard (NAAQS-2012) of China (Ministry of Environmental Protection of China, 2012), the grade II threshold of the maximum daily 8-h average (MDA8) of O_3 was 160 μg/m^3 (~75 ppbv). Two O_3 pollution events were found over 160 μg/m^3, which were named Case 1 (8th-17th Jun.) and Case 2 (20th-27th Jun.). Meanwhile, there were also O_3 pollution events on 6th Jun. and 29th-30th Jun. However, for better data coverage, we only discussed periods of O_3 pollution that lasted at least a week, and processes with relatively few days of pollution were not discussed in this study. The rest of the observation periods were clean days. Figure 1 shows the time series of the concentrations of TNMVOCs, O_3 8-h moving average, SO_2, $PM_{2.5}$, NO_x, CO, meteorological parameters (WD, WS, T, and RH), and from 1st to 30th June 2023. The gray areas in Fig. 1 are O_3 pollution events, and the remaining areas are clean days. During the observation, O_3 polluted days were 21 days, accounting for 70%.

During the observation period, the average wind speed (1.3 ± 0.9 m/s) was relatively low, which was not conducive to the dispersion. The mean RH (52 ± 19%) was low, and the mean temperature (28.9 ± 4.6 °C) was high. The meteorological conditions of high temperature and low RH were conducive to the occurrence

of photochemical pollution. The maximum daily 8-h moving average (MDA8) of O_3 reaching 229 μg/m^3. Hourly average concentrations of SO_2, NO_2, CO, and $PM_{2.5}$ were 4.4 ± 3.3 μg/m^3, 26.5 ± 17.9 μg/m^3, 0.6 ± 0.2 mg/m^3, 59.6 ± 26.5 μg/m^3 and 22.9 ± 7.1 μg/m^3, respectively. The concentrations of these pollutants were 97%, 87%, 94%, and 35% lower than the grade I threshold of the NAAQS-2012. The average concentration of TNMVOCs was 22.8 ± 8.3 ppbv.

During the Case 1 process, O_3 pollution continued for 10 days. The average RH and temperature were 41 ± 16% and 29.9 ± 4.1 °C, respectively, and the average WS was 1.3 ± 0.8 m/s. The concentration of MDA8 O_3 reached a maximum of 228 μg/m^3 (June 11) during the pollution period, which was higher than the grade II threshold of MDA8 O_3. In Case 1, the mean concentrations of SO_2, NO_2, CO, PM_{10} and $PM_{2.5}$ were 6.1 ± 4.1 μg/m^3, 27.4 ± 19.5 μg/m^3, 0.6 ± 0.1 mg/m^3, 69.1 ± 31.5 μg/m^3 and 25.6 ± 6.8 μg/m^3, respectively. The average concentration of TNMVOCs during this process was 24.1 ± 8.9 ppbv. In Case 2, O_3 pollution occurred continuously for 8 days. The average RH and average temperature were 50 ± 14% and 31.2 ± 2.9 °C. The average concentrations of TNMVOCs (22.5 ± 7.4 ppbv), SO_2 (2.7 ± 2.1 mg/m^3), NO_2 (24.9 ± 12.3 mg/m^3), CO (0.6 ± 0.1 mg/m^3), PM_{10} (61 ± 19 mg/m^3), and $PM_{2.5}$ (24 ± 7 mg/m^3) in Case 2 were all lower than those in Case 1 process.

The average concentrations of TNMVOCs, NO_2, PM_{10}, and $PM_{2.5}$ on clean days were lower than those of the O_3 pollution events. The average RH (65 ± 17%) on clean days was higher than those during Case 1 and Case 2 events, while the average temperature (26.0 ± 4.8 °C) was lower than those during Case 1 and Case 2 events. According to the analysis in Fig. S3a and Fig. S3b, O_3 has a significant correlation with temperature and RH, with correlation coefficients of 0.7 and -0.61 respectively. Therefore, conditions of high temperature and low RH are more conducive to O_3 pollution. Fig. S3c indicates that O_3 concentration exceeding the secondary standard mainly occurs under meteorological conditions of high temperature (greater than 30 °C) and low RH (less than 55%). It can be noted that when 35 °C < T < 40 °C and 20% < RH < 40%, the O_3 concentration consistently exceeds the grade II threshold of the NAAQS-2012. High temperature and low RH are more conducive to O_3 pollution (Chen et al., 2020; Zhang et al., 2015). Meng et al. (2023) argued that most of the reactions involved in O_3 formation increase with temperature, and the rate of O_3 production exceeds that of O_3 loss by a large margin. Therefore, during the study period, the meteorological conditions of high temperature and low RH are also important factors affecting the occurrence of O_3 pollution.

Besides, the average concentration of NO_2 in clean days (24.4 ± 16.1 ppbv) was lower than that in Case 1 and Case 2, while the average concentration of NO in clean days (4.8 ± 5.5 ppbv) was higher than that in Case 1 (3.9 ± 3.75 ppbv) and Case 2 (3.9 ± 2.4 ppbv). Higher concentration of NO_2 can promote the formation of O_3,

while the titration reaction between NO and O_3 consumes O_3 (Sillman, 1999). Therefore, the higher concentration of NO_2 and lower concentration of NO during pollution events are one of the reasons for the occurrence of O_3 pollution events.

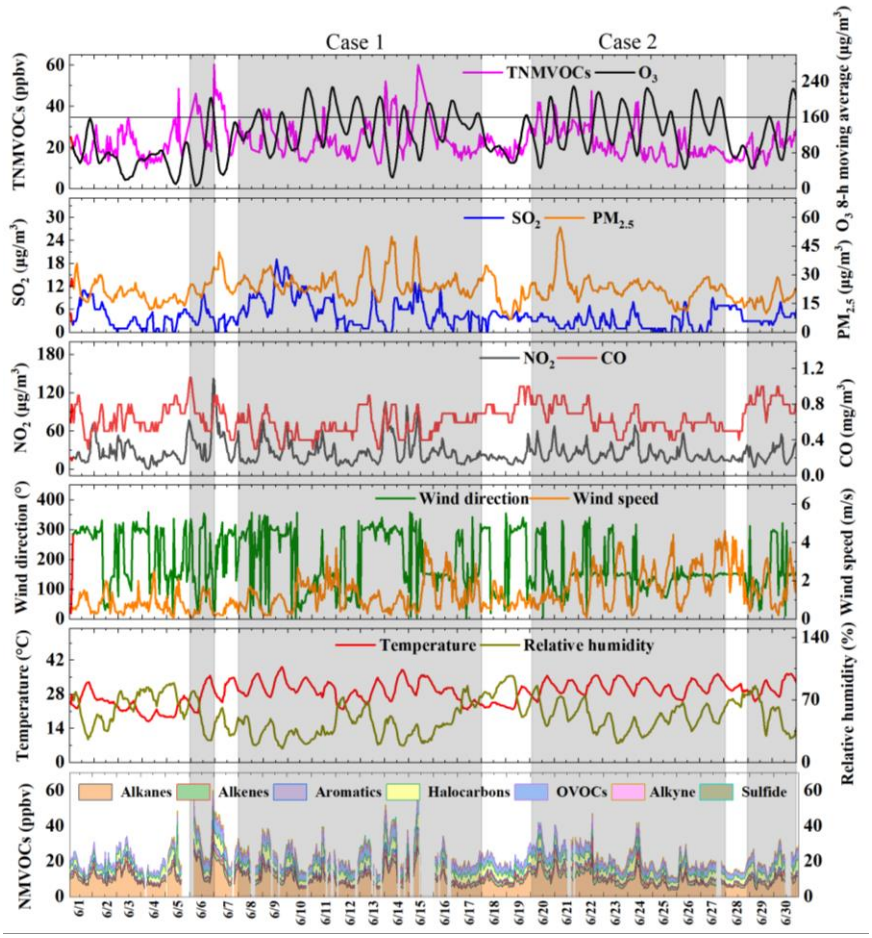

Figure 1. Hourly concentrations of TNMVOCs, O_3 8-h moving average, SO_2, $PM_{2.5}$, NO_2, CO, meteorological parameters (WD, WS, T, and RH), and NMVOCs during the sampling period (gray regions represent O_3 pollution processes).

The means and standard deviations of NMVOCs groups during different processes were listed in Table 1. During the entire period, the concentration of TNMVOCs varied from 10 to 60 ppbv, with an average concentration of 23.0 ± 8.0 ppbv. Similar levels of NMVOCs concentrations were observed between Case 1 (24.0 ± 9.0 ppbv) and Case 2 (23.0 ± 7.0 ppbv). The TNMVOCs concentrations on clean days were relatively low (21 ± 7.2 ppbv). Furthermore, nearly all NMVOCs groups in O_3 pollution events were higher than those on clean days.

As for the entire sampling period, alkanes (10.0 ± 4.4 ppbv), OVOCs (4.5 ± 1.3 ppbv), and halocarbons (4.3 ± 1.9 ppbv) were the most abundant NMVOCs groups, accounting for 44, 20 and 19% of the TNMVOCs, respectively, followed by alkenes (9%), aromatics (5%), alkenes (5%), OVOCs (7%), alkyne (7%) and sulfide (1%). During the two O_3 pollution events, alkanes being the highest NMVOCs group contributed 41% (Case 1), and 43% (Case 2) to the TNMVOCs, respectively. Alkanes were the most abundant NMVOCs during the

observation period, in part due to the presence of alkanes emission sources around the observation site (e.g., civilian combustion and motor vehicle emissions) and the low photochemical reactivity of alkanes (Mozaffar et al., 2020). Even on clean days, alkanes (9.6 ± 3.9 ppbv) were also the highest group (46%), and halocarbons (19%) and OVOCs (19%) were another two major groups.

Table 1. Concentrations of NMVOCs during different processes in Zhengzhou, ppbv.

Species	Entire period (n = 652)		Case 1 Jun. 8 - 17 (n = 201)		Case 2 Jun. 20 - 27 (n = 184)		Clean days (n = 224)	
	Range	Average ± SD	Range	Average ± SD	Range	Average ± SD	Range	Average ± SD
Alkanes	3.6 - 30.7	10.0 ± 4.4	4.2 - 28.3	10.0 ± 4.6	3.6 - 24.6	9.6 ± 4.1	4.6 - 22.2	9.6 ± 3.9
Alkenes	0.4 - 10.7	2.0 ± 1.2	0.6 - 10.7	1.9 ± 1.2	0.6 - 10.7	2.5 ± 1.4	0.4 - 4.0	1.7 ± 0.7
Aromatics	0.3 - 5.0	1.1 ± 0.7	0.4 - 4	1.2 ± 0.8	0.3 - 3.1	1.1 ± 0.6	0.3 - 4.4	1.1 ± 0.6
Halocarbons	1.8 - 31.1	4.3 ± 1.9	2.0 - 10.6	4.5 ± 1.8	2.2 - 8.8	4.2 ± 1.4	1.8 - 31.1	3.9 ± 2.2
OVOCs	1.8 - 9.7	4.5 ± 1.3	3.4 - 9.7	5.3 ± 1.2	2.0 - 8.1	4.4 ± 1.1	1.8 - 8.6	3.9 ± 1.2
Sulfide	0.0 - 1.5	0.1 ± 0.2	0.0 - 1.5	0.2 ± 0.3	0.0 - 0.5	0.1 ± 0.1	0.0 - 1.0	0.1 ± 0.1
Alkyne	0.1 - 3.7	1.1 ± 0.6	0.2 - 3.2	1.1 ± 0.6	0.2 - 3.2	1.0 ± 0.5	0.1 - 3.7	1.0 ± 0.7
TNMVOCs	9.9 - 60.3	22.8 ± 8.3	0 - 60.0	24.1 ± 8.9	10.5 - 47.3	22.5 ± 7.4	9.9 - 48.5	20.8 ± 7.2

n: Total sampling numbers for each process

Figure 2 illustrates the fifteen NMVOCs with the highest average mixing ratio during two O_3 pollution events and clean days. Ethane, propane, n-butane, isopentane, isobutane, n-hexane, and n-pentane were the most abundant of the alkanes during each of the entire observation period. Ethane is a major component of natural gas (NG) (Thijsse et al., 1999), propane, n-butane, and isobutane are important tracers of liquefied petroleum gas (LPG) (Tsai et al., 2006; An et al., 2014). N-hexane is mainly from solvent emissions. Ethylene, propylene, and isoprene were the most abundant of the alkenes. Ethylene and propylene mainly come from biomass burning (Andreae and Merlet, 2001). Isoprene mainly comes from plants (Brown et al., 2007). Acetylene also had a high level, which is the tracer of incomplete combustion (Blake and Rowland, 1995). Benzene and toluene were the most abundant of the aromatics, which are mainly from solvent emissions, vehicular exhaust, and industry processes (Seila et al., 2001; Mo et al., 2015). Dichloromethane was the most abundant species of the halohydrocarbons, which is an important species in solvent usage (Huang et al., 2014). The acetone was the most abundant species in OVOCs, which has complex atmospheric sources and is mainly attributed to vehicular emission and secondary formation (Guo et al., 2013; Watson et al., 2001). The concentration of acetone in the two pollution processes was significantly higher than that in the clean day as also reported by others (Guo et al., 2013), indicating that the pollution process had a strong photochemical reaction e.g., photo-oxidation of i-butene to acetone (Guo et al., 2013). Therefore, vehicle exhaust, solvent use, combustion, biogenic emission, and industrial processes are important sources of NMVOCs at observation sites, as also illustrated in the following PMF source apportionment (in section 3.2.2).

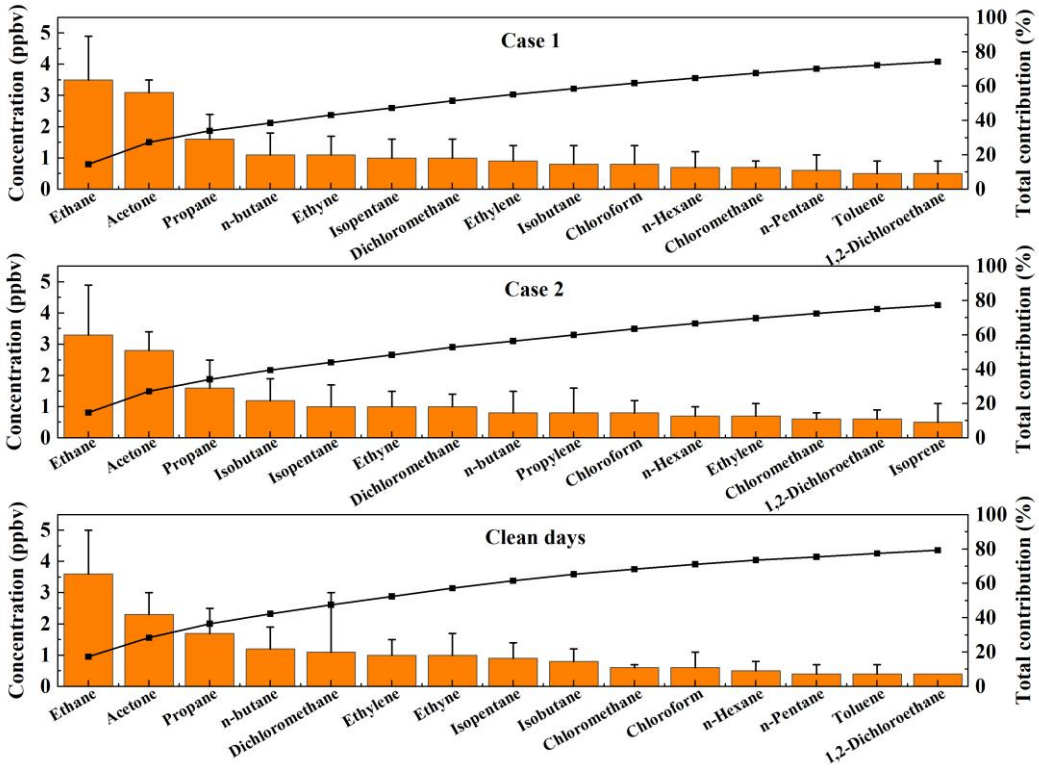

Figure 2. Comparisons of the fifteen NMVOCs with the highest average mixing ratio during different processes, ppbv. Error bars are standard deviations.

3.1.2 Diurnal variations of NMVOCs, O_3, and NO_x

The concentration characteristics of pollutants in the atmosphere are affected by the atmospheric boundary layer variation pattern, photochemical reaction intensity, and emission of pollution sources (Wang et al., 2023a). A selection of NMVOCs, O_3, and NO_x were selected, and their daily changes were analyzed, as shown in Fig. S4. The diurnal variation of O_3 concentration shows unimodal characteristic. During the day, with the increase in temperature and light intensity, the concentration of O_3 gradually increased and reached a peak at about 14:00, and then the concentration gradually decreased. This diurnal pattern is influenced by strong photochemical reactivity, boundary layer processes, and meteorological parameters. Higher O_3 production during the day indicates significant contributions from both photochemical reactions and atmospheric mixing processes. The diurnal variation of ethane, propane, isobutane, n-butane, isopentane, n-pentane, ethylene, propylene, acetylene, benzene, and toluene were similar, showing low concentrations in the daytime and high concentrations in the evening. This is associated with a higher boundary layer and strong photochemical reactivity during the day (Tang et al., 2007). The elevated boundary layer is conducive to the dispersion of NMVOCs and other pollutants (Bon et al., 2011; Chen et al., 2022a), while the strong photochemical reaction will consume NMVOCs (Xia et al., 2014; Zhang et al., 2018). In addition, the peak concentrations of these NMVOCs were observed in the morning and evening (7:00-8:00 and 23:00-24:00), showing a consistent daily pattern with NO_x. This suggests that the emissions of these NMVOCs are significantly influenced by motor

vehicle emissions and fuel combustion. Higher NMVOCs and NO_x concentrations at night may be caused by heavy traffic emissions for traditional nighttime activities in the city. Isoprene is a typical tracer of plant emissions, which are highly dependent on temperature and solar radiation (Guenther et al., 1993; Sharkey et al., 1996). Therefore, the concentration of isoprene increases significantly during the day (7:00-20:00) and decreases significantly at night. It is worth noting that the concentration of isoprene showed a bimodal characteristic. Two peaks occur at 10:00 AM and 15:00 PM (local standard time). Previous studies have shown that the rate at which plants emit isoprene decreases when temperatures exceed 40 ℃ (Guenther et al., 1993; Sharkey et al., 1996). Therefore, the drop in isoprene concentrations seen at noon may be due to excessive temperatures affecting biogenic emissions. Additionally, the concentration of OH radicals peaks at noon (Fig. S5), leading to the rapid oxidation of isoprene by OH radicals, which further contributes to the observed bimodal pattern (Paulot et al., 2009). Acetone comes from a wide range of sources, mainly from vehicle emissions, industrial production, and secondary formation (Sha et al., 2021). Acetone remained in high concentration throughout the day, and there was no obvious diurnal variation, suggesting that there might be primary acetone sources near the site, which concealed the acetone peak at the daytime produced by photochemical reaction (Guo et al., 2013). Dichloromethane mainly comes from solvent use, and its high concentration was mainly concentrated at night (23:00-5:00), which might be related to the longer atmospheric lifetime of dichloromethane and the lower boundary layer height at night (Li et al., 2018; Chen et al., 2022a).

3.2 Sources of NMVOCs

3.2.1 Diagnostic ratios

Ratios of specific NMVOCs can be used to assess the initial emission source of NMVOCs or the degree of photochemical reaction (Miller et al., 2012; An et al., 2014). The ratios of isopentane/n-pentane, toluene/benzene (T/B), and m-p-xylene/ethylbenzene (E/X) are discussed in this study (Fig. 3).

In Case 1, Case 2, and clean days, the Pearson coefficients of isopentane and n-pentane were 0.7, 0.94, and 0.6, respectively, indicating a strong correlation that the two substances had a common emission source. Isopentane/n-pentane ratios of 0.8-0.9, 2.2-3.8, 1.5-3.0 and 1.8-4.6 (Fig. 3a), indicate that isopentane and n-pentane come from natural NG, vehicle emissions, liquid gasoline, and fuel evaporation, respectively (An et al., 2014; Watson et al., 2001). In this study, the ratios of Case 1, Case 2, and clean days were 0.7, 2.5, and 1.1, respectively. It suggests that isopentane and n-pentane may come from NG emissions, vehicular exhaust, and liquid gasoline, respectively.

The T/B ratio can be used to distinguish between coal and biomass combustion (0.2-0.6), motor vehicle emissions (~2.0) (Liu et al., 2008), industrial processes (3.0-6.9) (Zhang et al., 2016) and fuel evaporation

(~4.1) (Dai et al., 2013). In this study, the T/B ratio of the two O_3 pollution events was 1.7 and 1.4 (Fig. 3b), respectively, indicating that combustion and vehicle emissions were the main sources of benzene and toluene emissions (Hong et al., 2019).

Since m/p-xylene and ethylbenzene share a common source but differ in their OH radical reaction rate constants, the E/X ratio can be used to understand source characteristics (Miller et al., 2012; Yurdakul et al., 2018). During the pollution events and clean days, m, p-xylene, and ethylbenzene showed a strong positive correlation (r = 0.9) (Fig. 3c), indicating that m/p-xylene and ethylbenzene came from a common emission source. Previous studies have shown that NMVOCs are transported from inner urban areas when the E/X ratio is 0.3-0.4, and NMVOCs are transported from distant sources when the ratio is significantly higher than 0.3 (Monod et al., 2001). In this study, the E/X ratios of the two pollution events and clean days were 0.5, indicating that the air mass measured at the observation point was affected by air mass transport. We have analyzed the relationship between ethylbenzene, m/p-Xylene, E/X, and wind direction and speed. As shown in Fig. S6, the concentrations of ethylbenzene and m/p-Xylene are mainly influenced by winds coming from the northwest, and their concentrations tend to increase with stronger wind speeds. Similarly, E/X also exhibits similar patterns of variation, further indicating the regional transport of ethylbenzene and m/p-xylene from distant sources.

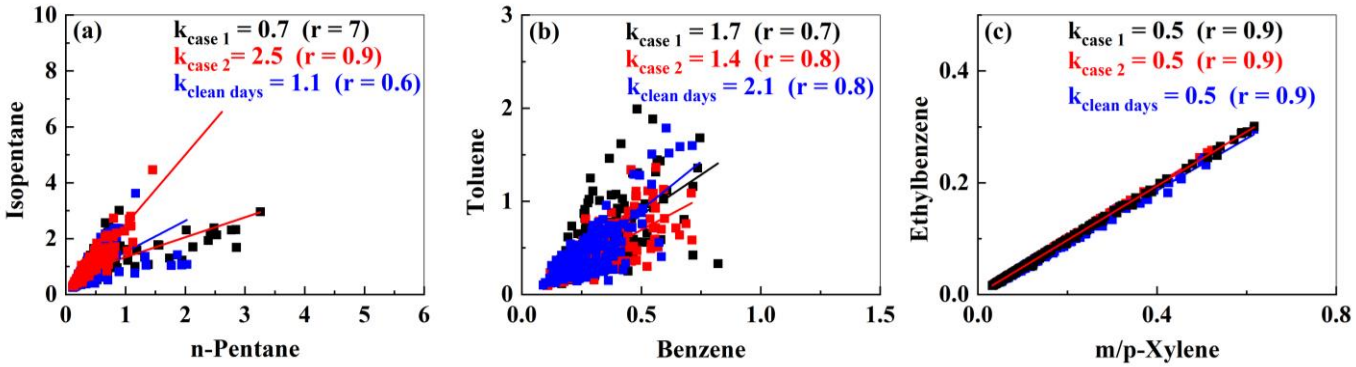

Figure 3. Correlations (k = slope) between compounds with different observation periods.

3.2.2 Source apportionment

In this study, EPA PMF5.0 was used to analyze the source profile and species percentage of each source during the observation period to determine the relative contribution of each potential source, as shown in Fig. 4. Seven factors were determined by the model, namely combustion, industrial production, biogenic emission, vehicular exhaust, LPG/NG, solvent use 1, and solvent use 2. Detailed analysis is followed.

Factor 1 was characterized by high percentages of acetylene (76%), ethane, propane, ethylene benzene, and toluene. Acetylene is a typical tracer of coal burning (Barletta et al., 2005). Ethane, propane, and ethylene are typically tracers of incomplete combustion (Guo et al., 2011; Ling et al., 2011). Therefore, Factor 1 was

classified as combustion. The CPF plots indicate that the contributing direction was northwest at about 2 m/s (Fig. S7a).

Factor 2 was rich in C4-C6 alkanes, aromatics, (toluene, ethylbenzene, m/p-Xylene, o-xylene, and 1,2,4-trimethylbenzene, and halocarbons (1, 2-dichloroethane and 1, 2-dichloropropane). Previous studies have shown that these species were all related to industrial production. Therefore, Factor 2 was classified as industrial production. The CPF plots indicated that a local source under a low wind speed of < 1 m/s was the dominant source (Fig. S7b).

Factor 3 was characterized by high percentages (83%) of isoprene, a typical tracer of biogenic emission (Brown et al., 2007). The high temperature and strong radiation in summer are more conducive to the biogenic emission of isoprene (Liu et al., 2016). Therefore, Factor 3 was classified as a biogenic emission. The CPF plots indicated that the southwest was the dominant source direction under wind speeds below 2 m/s (Fig. S7c).

Factor 4 was characterized by high percentages of C2-C6 alkanes (such as ethane, propane, isobutane, n-butane, isopentane, n-pentane, 2, 2-dimethylbutane, and 2, 3-dimethylbutane), benzene, toluene, ethylbenzene, and m/p-xylene), which are related to vehicular emission (Jorquera and Rappenglück, 2004; Song et al., 2007; Chen et al., 2014). Therefore, Factor 4 was classified as vehicular exhaust. The CPF plots indicated that a local source under a low wind speed was the dominant source, which might be related to the large amount of traffic on the main roads in the southern and western directions direction (Fig. S7d).

Factor 5 was characterized by high percentages of ethane, propane, isobutane, and propylene, which are the main components of LPG/NG (Shao et al., 2016; Song et al., 2007; Na et al., 2001). Therefore, Factor 5 was classified as LPG/NG source. The CPF plots showed the dominant source directions of this factor were east at 1-2 m/s (Fig. S7e).

Factor 6 was characterized by high percentages of chloromethane, dichloromethane, tetrachloromethane, 1,2-dichloroethane, 1,2-dichloropropane, and ethyl acetate, which are typical solvents for industrial applications (Li et al., 2020; Huang et al., 2014). Therefore, Factor 6 was assigned to solvent usage 1. The CPF plots of this factor indicated that the northeast and southeast were the dominant directions (Fig. S7f).

The Factor 7 was dominated by methylcyclopentane, cyclohexane, TEXs（Toluene, Ethylbenzene, m/p-Xylene, and o-Xylene）, 1,2-Dichloroethane、1,2-Dichloropropane, and Ethyl acetate. Methylcyclopentane and cyclohexane were commonly used as solvents in industrial processes (Lyu et al., 2016; Yuan et al., 2013). TEX is the main component of organic solvents (Guo et al., 2011; Watson et al., 2001). Therefore, Factor 7 was assigned to solvent usage 2. The CPF plots of this factor indicate that the high CPF values were found

near the center when the wind speed was low (≤1 m/s).This finding indicates that local emissions was the dominant source (Fig. S7g).

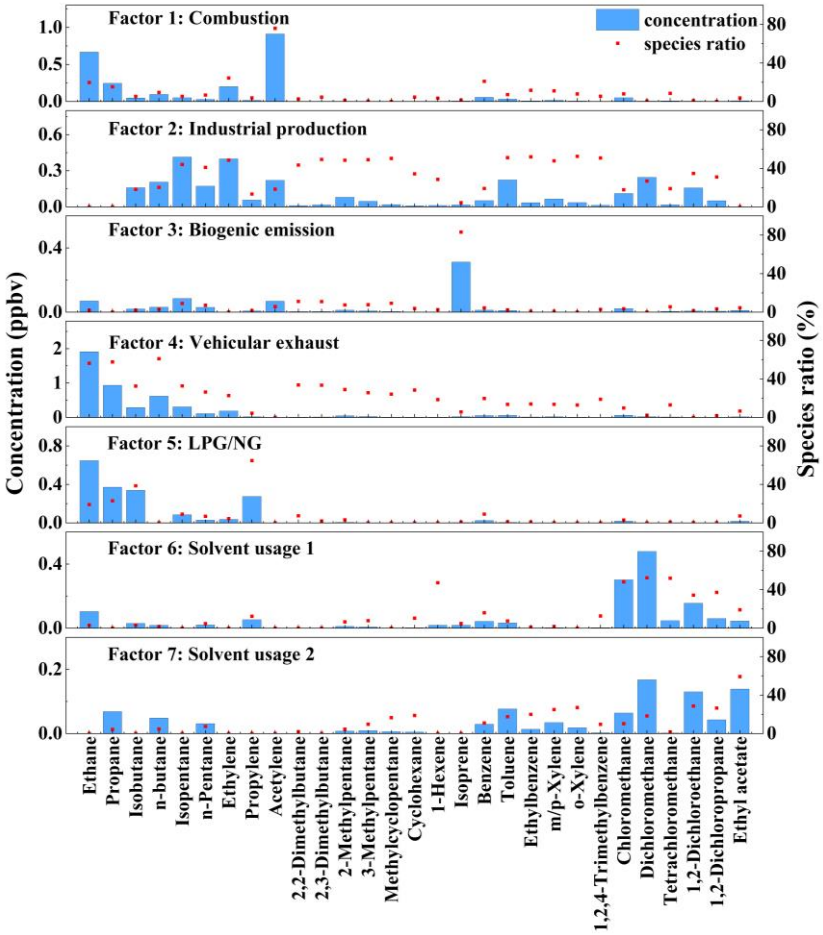

Figure 4. Source profiles and contributions of NMVOCs during the observation period.

Figure 5 shows the proportion of each NMVOCs source during the observation process. In the entire observation period, vehicular exhaust is the main contributor, accounting for 28%, followed by solvent usage (27%) and industrial production (22%). Other sources including LPG/NG (9%), combustion sources (8%), and biogenic emission (6%) contributed little. In Case 1, vehicular exhaust (30%) was the largest contributor, followed by solvent usage (27%) and industrial production (23%). Compared with the Case 1 event, the contribution of solvent usage and industrial production in the Case 2 event did not change much, and the contribution of LPG/NG increased by 14%, which became an important source. On clean days, vehicular exhaust (35%), solvent usage (25%), and industrial production (21%) were the most significant contributors. Compared with clean days, the contribution of solvent usage, industrial production, biogenic emission, and LPN/NG in both pollution events increased, while the contribution of combustion sources and vehicular exhaust decreased. In summary, vehicular exhaust, solvent usage, and industrial production were major contributors to both O_3 pollution events and clean days.

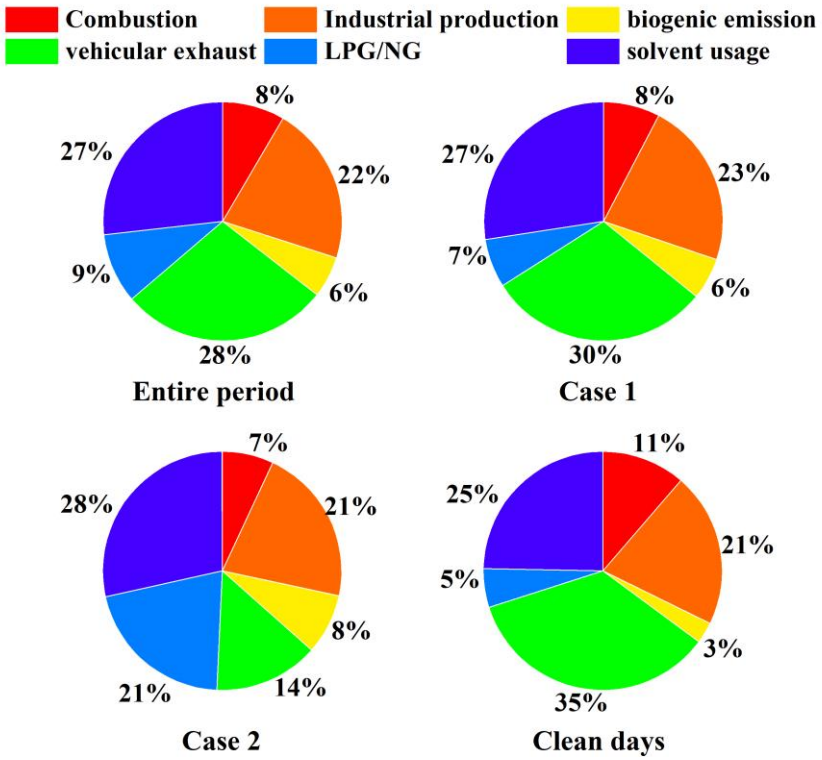

Figure 5. Source contributions to NMVOCs concentrations during different periods.

In summary, the observation sites are significantly influenced by vehicular exhaust, solvent usage, and industrial production. The results of this study show similarities in the source apportionment of NMVOCs in Zhengzhou during the summers of 2018 to 2021 (Yu et al., 2022; Guo et al., 2024). Yu et al. (2022) found that vehicular exhaust and industrial production contributed the most to NMVOCs emissions in Zhengzhou from 2018 to 2020, with the main sources of summer NMVOCs being vehicular exhaust, solvent usage, and industrial production. In contrast to the NMVOCs source apportionment results of Li et al. (2021). for the O_3 pollution process in Zhengzhou in May 2018, the difference lies in the higher impact of solvent usage compared to vehicular exhaust and industrial production. This is mainly attributed to the fact that Li et al. (2021)'s observation site was located within Zhengzhou University, making them more susceptible to the influence of chemical reagent use. In comparison to the source apportionment of NMVOCs in Zhengzhou during winter (Zhang et al., 2021), combustion also becomes an important contributor during winter, attributed to the increased heating demand, while the contribution from solvent usage is relatively lower due to the cold temperatures. In comparison with other cities (Table S3), vehicular exhaust in Zhengzhou contributes the most, higher than in cities such as Qingdao (Wu et al., 2023), Xuchang (Qin et al., 2021), Guangzhou (Meng et al., 2022), Nanjing (Fan et al., 2021), Shijiazhuang (Guan et al., 2020), and Weinan (Hui et al., 2020), but lower than in Changzhou (Liu et al., 2023) and on par with Beijing (Liu et al., 2020). Solvent usage in Zhengzhou contributes more than in Qingdao (Wu et al., 2023), Xuchang (Qin et al., 2021), Nanjing (Fan et al., 2021), Shijiazhuang (Guan et al., 2020), Weinan (Hui et al., 2020), Changzhou (Liu et al., 2023), and Beijing (Liu et

al., 2020), but less than in Guangzhou (Meng et al., 2022). Industrial production in Zhengzhou contributes more than in Xuchang (Qin et al., 2021), Guangzhou (Meng et al., 2022), Nanjing (Fan et al., 2021), Weinan (Hui et al., 2020), and Changzhou (Liu et al., 2023), but less than in Shijiazhuang (Guan et al., 2020).

3.3 Contribution to O_3 formation

3.3.1 O_3 sensitivity analysis

In this study, the RIR of AVOCs, BVOCs, CO, NO_x, alkanes, alkenes, and aromatics were calculated (Fig. 6). The RIR values of NMVOCs were all positive during the entire period, indicating that O_3 generation is most sensitive to NMVOCs reduction. In comparison, the RIR value of NO_x was negative, indicating that reduction of NO_x would cause the increasing of the O_3 concentration. Among AVOCs, aromatics had the highest RIR value, followed by alkenes and alkanes. For both O_3 pollution events and clean days, the RIR value of NO_x was negative, and the RIR of NMVOCs and CO were positive. In pollution events, apart from BHC, the absolute values of RIR for each group and species are lower than those in clean days, indicating that the sensitivity of O_3 to NMVOCs, NO_x, and CO on clean days was higher than that in the O_3 pollution events. Compared to clean days, during ozone pollution events, the RIR value of AVOCs decreased by 11%, with Aromatics showing the largest decrease (26%), while Alkanes and Alkenes increased by 7% and 3% respectively. Additionally, in pollution events, CO and NO_x were reduced by 41% and 18%, respectively. Additionally, CO and NOx decreased by 29% and 22%.

Isoprene was the sole BVOC considered in this study. Isoprene is an important tracer to indicate biogenic emissions (Xie et al., 2021; Li et al., 2024; Qin et al., 2023). During the entire period, especially in the pollution events, the RIR of AVOCs was lower than that of BVOCs, indicating that O_3 formation was more sensitive to biogenic emissions. This may be due to increased emissions of BVOCs at higher temperatures and solar radiation conditions, as well as their high reactivity and O_3 formation potential. Studies in Yucheng (Zong et al., 2018), Leshan (Xie et al., 2021), and and Nanjing (Fan et al., 2021; Ming et al., 2020) have shown that O_3 is highly sensitive to BVOCs. Studies in Zhengzhou (Wang et al., 2022), Hangzhou (Zhao et al., 2020), and Hong Kong (Wang et al., 2017) suggested that O_3 exhibits greater sensitivity to BVOCs than AVOCS during hot seasons. Wang et al. (2019) found in their study on O_3 source apportionment in Henan Province, where Zhengzhou is located, that BVOCs contribute to approximately 23.9% of the O_3 attributed to NMVOCs. Therefore, the contribution of BVOCs to O_3 is very important.

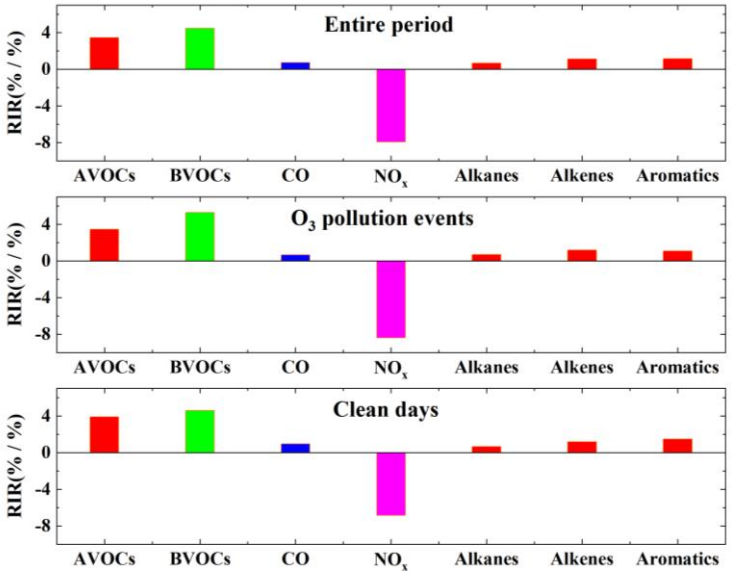

Figure. 6. Average RIR values of the O_3 for different species/groups during different processes in Zhengzhou.

3.3.2 Empirical kinetics modeling approach (EKMA) results

Given the current inability to implement appropriate control measures for BVOCs, the following analysis considers only the impact of AVOCs and NO_x on O_3 formation. The EKMA curve drawn based on the OBM model is shown in Fig. 7. It can be seen from the EKMA curve that O_3 generation presents a highly nonlinear relationship with its precursor compounds AVOCs and NO_x, and the same O_3 concentration can be generated by different concentration combinations of AVOCs and NO_x. In the figure, AVOCs and NO_x = 100% is the base case, and the horizontal and vertical axes represented the percentages of AVOCs and NO_x relative to the actual observed mixture ratio (100%). The straight lines in the figure are called ridgeline and is formed by the junction of turning points of O_3 concentration lines (Dodge, 1977).

The ridge divides the graph into the upper left and the lower right parts, and there are also large differences in O_3 generation between these two parts. In the lower right part, each O_3 concentration line and the horizontal coordinate show a parallel relationship. If the NO_x concentration was maintained unchanged, the O_3 concentration does not change with the change of AVOCs concentration. When the AVOCs concentration is unchanged, the concentration of O_3 decreases with the decrease of NO_x concentration. Therefore, in this part of the region, O_3 generation is controlled by NO_x. In the upper left part, if the concentration of AVOCs is reduced alone, the concentration of O_3 will decrease significantly; if only the concentration of NO_x is reduced, the concentration of O_3 will first rise and then decrease. In this region, O_3 generation is in the control region of AVOCs. In the area near the ridge line, when NO_x and AVOCs are reduced at the same time, the O_3 concentration will decrease, and the O_3 generation in the cooperative control area of AVOCs and NO_x.

The ridgeline slope of this EKMA curve was about 6:1, that was, the reduction of NO_x and AVOCs along this ridge was the fastest way to reduce the O_3 concentration. As can be seen from the figure, Zhengzhou was a

typical AVOCs control area, and O_3 was very sensitive to the changes of AVOCs. At the same time, Case 1, Case 2, and clean days are all above the ridgeline and belong to the AVOCs control region (Fig. S8). Therefore, reducing AVOCs can effectively reduce the generation of O_3.

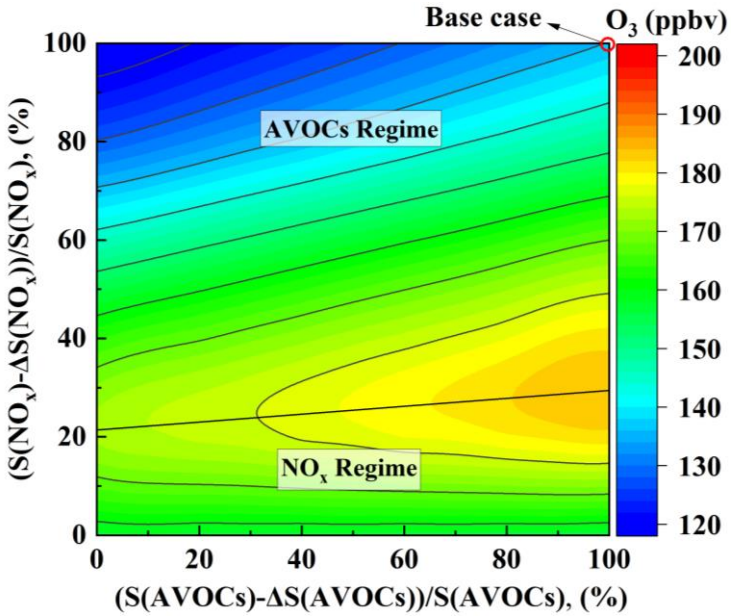

Figure 7. Isopleth diagram of modeled O_3 on S(AVOCs) and S(NO_x) remaining percentages.

3.3.3 Control strategies of O_3

The above analysis based on single species (NO_x or AVOCs) is only used to discuss the sensitivity of O_3 concentration to precursor, but such extreme control is difficult to achieve. Usually in the actual operation, the method of simultaneously controlling NO_x and AVOCs emissions is usually adopted to reduce the concentration of O_3. To establish a reasonable and effective AVOCs and NO_x emission reduction plan, we further conducted a series of simulations to calculate the O_3 concentration by adjusting the ratio of input AVOCs and NO_x. The following analyzes the reduction cases of O_3 control at 10 a.m. to 4 p.m. during the observation period.

Figure 8 shows different reduction schemes. In Fig. 8, the horizontal and vertical axes corresponded to the reduction percentages of NO_x or NO_x + AVOCs and the reduction percentage of O_3 concentration (positive and negative values represent the increase and decrease of O_3 concentration compared to the base case). The results show that O_3 concentration will eventually decline regardless of the reduction method, but the trend of change (Fig. 8a). As can be seen from Fig. 8b, if only NO_x was reduced, when the emission reduction was less than 60%, the change in O_3 concentration shows an increasing trend; when the emission reduction was greater than 60%, the change of O_3 concentration shows a decreasing trend. Therefore, only NO_x emission reduction was not conducive to the reduction of O_3 concentration. When the reduction ratio of AVOCs/NO_x was 1:2 and 1:1, the change in O_3 concentration shows a similar trend as that of NO_x emission reduction only, and O_3

concentration increases first and then decreases. When the reduction ratio of AVOCs/NO_x was 2:1, O_3 concentration increases to a certain extent. When the emission reduction ratio of AVOCs/NO_x was 3:1 or 4:1, O_3 concentration continues to decline, and the decline rate of O_3 concentration of 4:1 was greater than 3:1. If only AVOCs emissions were reduced, O_3 concentration shows a continuous downward trend, and the decline rate was very fast. However, combined with actual production activities, only reducing AVOCs emissions cannot be achieved, which was not conducive to policy implementation. Therefore, from the perspective of comprehensive emission reduction effect, the reduction ratio of AVOCs/NO_x should be no less than 3:1, which will be conducive to the reduction of O_3 concentration.

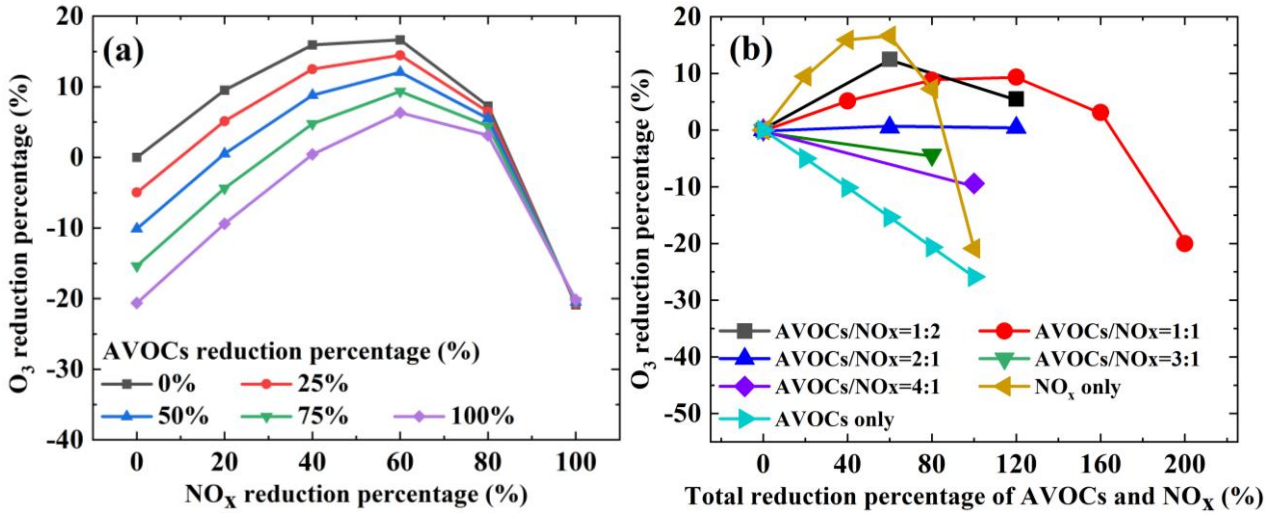

Figure 8. Response of the O_3 concentration to different AVOCs and NO_x reduction percentages. Note: AVOCs/NO_x was the ratio of the percentage reduction of AVOCs and NO_x.

In addition, this study analyzed O_3 reduction schemes from 10 a.m. to 4 p.m. It can be seen from Fig. S9 that with the reduce of NO_x, O_3 concentration elevated and then decreased. When the reduction ratio of AVOCs was fixed and the reduction ratio of NO_x was less than 60%, O_3 concentration increases with the reduce of NO_x. In this case, O_3 concentration increased by 30, 21, 16, 13, 13, 15, and 15% from 10 a.m. to 4 p.m. (that is, under the AVOCs scenario without reduction). When the NO_x reduction ratio was greater than 60%, O_3 concentration decreases with the reduce of NO_x. When the reduction was the greatest (that is, 100% reduction of NO_x and AVOCs), O_3 concentration at 10 o 'clock was still increased compared with the atmospheric observation concentration, increased by 14%; O_3 concentration at 11 a.m. to 4 p.m. decreased by 2, 15, 25, 32, 36, and 36%, respectively.

Between the range of 10 a.m. to 4 p.m. in the day, when only NO_x was reduced, O_3 concentration elevated and then decreased. When only AVOCs were reduced, O_3 concentration continued to decrease. When the reduction ratio of AVOCs/NO_x was less than 2:1, O_3 concentration elevated and then decreased. When the reduction ratio of AVOCs/NO_x was greater than 2:1, O_3 concentration continues to decrease. When AVOCs/NO_x = 4:1,

O_3 concentration decreases the most and the fastest. According to the reduction ratio of AVOCs/NO_x = 4:1, the maximum reduction of O_3 concentration at 10 a.m. to 4 p.m. during the day were 3, 6, 10, 11, 13, and 13%, respectively.

4 Conclusions

Summer O_3 pollution remains an important environmental issue in Zhengzhou. This study investigated the characteristics and emission sources of O_3 precursors from 1st to 30th June 2023. The OBM was used to analyze the influence of precursors on the formation of O_3, and the emission reduction strategy of precursors was proposed to control the concentration of O_3. During the entire period, the concentration of TNMVOCs varied from 9.9 to 60.3 ppbv, with an average value of 22.9 ± 8.3 ppbv. The average concentrations of TNMVOCs during O_3 pollution were higher than that during clean days. Alkanes (44%), OVOCs (20%), and halocarbons (19%) were the most abundant NMVOCs group. The most abundant species in both O_3 pollution events and clean days were ethane, acetone, and propane. The average concentrations of NO_2 in pollution events were higher than those in clean days, while the average concentrations of NO were lower than those in clean days. Therefore, the increasing concentrations of O_3 precursors were one of the reasons for the formation of O_3 pollution. At the same time, the unfavorable meteorological conditions of high temperature and low RH in the observation process are also important factors in the formation of O_3 pollution. Further analysis of the sources revealed that vehicular exhaust (28%), solvent usage (27%), and industrial production (22%) were the main emission sources of NMVOCs. The increase of solvent usage, biogenic emission and LPN/NG contribution is an important cause of O_3 pollution. Sensitivity analysis of O_3 to precursors found that NMVOCs had the highest RIR value, while NO_x had a negative RIR value. Alkenes have the highest RIR value among AVOCs. It should be noted that the RIR value of BVOCs was greater than that of AVOCs. The local O_3 formations were in the AVOC-limited regime, which means reducing the concentration of AVOCs was an effective way to reduce O_3 concentration. We recommend a minimum reduction ratio of AVOCs/NO_x of no less than 3:1 to effectively reduce O_3 formation.

Data availability. Data can be obtained upon request from the authors.

Authorship contributions. DZ performed chemical modelling analyses of OBM-MCM and wrote the paper. XL collected the data and contributed to the data analysis. RZ designed and revised the paper. QX, FS, and SW contributed to discussions of results. MY and YX provided part of the data in Zhengzhou.

Competing interests. The contact author has declared that neither they nor their co-authors have any

competing interests.

Financial support. This work was supported by National Key Research and Development Program of China (No. 2017YFC0212403).

References

An, J., Zhu, B., Wang, H., Li, Y., Lin, X., and Yang, H.: Characteristics and source apportionment of VOCs measured in an industrial area of Nanjing, Yangtze River Delta, China, Atmos. Environ., 97, 206-214, https://doi.org/10.1016/j.atmosenv.2014.08.021, 2014.

Andreae, M. O., and Merlet, P.: Emission of trace gases and aerosols from biomass burning, Global. Biogeochem. Cy., 15, 955-966, https://doi.org/10.1029/2000GB001382, 2001.

Barletta, B., Meinardi, S., Sherwood Rowland, F., Chan, C.-Y., Wang, X., Zou, S., Yin Chan, L., and Blake, D. R.: Volatile organic compounds in 43 Chinese cities, Atmos. Environ., 39, 5979-5990, https://doi.org/10.1016/j.atmosenv.2005.06.029, 2005.

Billionnet, C., Gay, E., Kirchner, S., Leynaert, B., and Annesi-Maesano, I.: Quantitative assessments of indoor air pollution and respiratory health in a population-based sample of French dwellings, Environ. Res., 111, 425-434, https://doi.org/10.1016/j.envres.2011.02.008, 2011.

Blake, D. R., and Rowland, F. S.: Urban Leakage of Liquefied Petroleum Gas and Its Impact on Mexico City Air Quality, Science, 269, 953-956, https://doi.org/10.1126/science.269.5226.953, 1995.

Bon, D. M., Ulbrich, I. M., de Gouw, J. A., Warneke, C., Kuster, W. C., Alexander, M. L., Baker, A., Beyersdorf, A. J., Blake, D., Fall, R., Jimenez, J. L., Herndon, S. C., Huey, L. G., Knighton, W. B., Ortega, J., Springston, S., and Vargas, O.: Measurements of volatile organic compounds at a suburban ground site (T1) in Mexico City during the MILAGRO 2006 campaign: measurement comparison, emission ratios, and source attribution, Atmos. Chem. Phys., 11, 2399-2421, https://doi.org/10.5194/acp-11-2399-2011, 2011.

Brown, S. G., Frankel, A., and Hafner, H. R.: Source apportionment of VOCs in the Los Angeles area using Positive Matrix Factorization, Atmos. Environ., 41, 227-237, https://doi.org/10.1016/j.atmosenv.2006.08.021, 2007.

Callén, M. S., Iturmendi, A., and López, J. M.: Source apportionment of atmospheric $PM_{2.5}$-bound polycyclic aromatic hydrocarbons by a PMF receptor model. Assessment of potential risk for human health, Environ. Pollut., 195, 167-177, https://doi.org/10.1016/j.envpol.2014.08.025, 2014.

Cardelino, C. A., and Chameides, W. L.: An observation-based model for analyzing ozone precursor

612 relationships in the urban atmosphere, J. Air. Waste. Manage., 45, 161-180,
613 https://doi.org/10.1080/10473289.1995.10467356, 1995.
614 Cardelino, C. A., and Chameides, W. L.: The application of data from photochemical assessment monitoring
615 stations to the observation-based model, Atmos. Environ., 34, 2325-2332, https://doi.org/10.1016/S1352-
616 2310(99)00469-0, 2000.
617 Carslaw, D. C., and Ropkins, K.: openair — An R package for air quality data analysis, Environ. Modell.
618 Softw., 27-28, 52-61, https://doi.org/10.1016/j.envsoft.2011.09.008, 2012.
619 Chameides, W. L., Fehsenfeld, F., Rodgers, M. O., Cardelino, C., Martinez, J., Parrish, D., Lonneman, W.,
620 Lawson, D. R., Rasmussen, R. A., Zimmerman, P., Greenberg, J., Middleton, P., and Wang, T.: Ozone
621 precursor relationships in the ambient atmosphere, J. Geophys. Res-Atmos., 97, 6037-6055,
622 https://doi.org/10.1029/91jd03014, 1992.
623 Chen, D., Xu, Y., Xu, J., Lian, M., Zhang, W., Wu, W., Wu, M., and Zhao, J.: The Vertical Distribution of
624 VOCs and Their Impact on the Environment: A Review, Atmosphere, 13, 1940,
625 https://doi.org/10.3390/atmos13121940, 2022a.
626 Chen, D., Zhou, L., Wang, C., Liu, H., Qiu, Y., Shi, G., Song, D., Tan, Q., and Yang, F.: Characteristics of
627 ambient volatile organic compounds during spring O_3 pollution episode in Chengdu, China, J. Environ.
628 Sci., 114, 115-125, https://doi.org/10.1016/j.jes.2021.08.014, 2022b.
629 Chen, L., Zhu, J., Liao, H., Yang, Y., and Yue, X.: Meteorological influences on $PM_{2.5}$ and O_3 trends and
630 associated health burden since China's clean air actions, Sci. Total. Environ., 744, 140837,
631 https://doi.org/10.1016/j.scitotenv.2020.140837, 2020.
632 Chen, W. T., Shao, M., Lu, S. H., Wang, M., Zeng, L. M., Yuan, B., and Liu, Y.: Understanding primary and
633 secondary sources of ambient carbonyl compounds in Beijing using the PMF model, Atmos. Chem. Phys.,
634 14, 3047-3062, https://doi.org/10.5194/acp-14-3047-2014, 2014.
635 Chu, W., Li, H., Ji, Y., Zhang, X., Xue, L., Gao, J., and An, C.: Research on ozone formation sensitivity based
636 on observational methods: Development history, methodology, and application and prospects in China, J.
637 Environ. Sci., 138, 543-560, https://doi.org/10.1016/j.jes.2023.02.052, 2023.
638 Dai, P., Ge, Y., Lin, Y., Su, S., and Liang, B.: Investigation on characteristics of exhaust and evaporative
639 emissions from passenger cars fueled with gasoline/methanol blends, Fuel, 113, 10-16,
640 https://doi.org/10.1016/j.fuel.2013.05.038, 2013.
641 Dodge, M. C.: Combined use of modeling techniques and smog chamber data to derive ozone-precursor
642 relationships, Proceedings of the International Conference on Photochemical Oxidant Pollution and Its

643 Control, 2, 881-889, 1977.
644 Fan, M., Zhang, Y., Lin, Y., Li, L., Xie, F., Hu, J., Mozaffar, A., and Cao, F.: Source apportionments of
645 atmospheric volatile organic compounds in Nanjing, China during high ozone pollution season,
646 Chemosphere, 263, https://doi.org/10.1016/j.chemosphere.2020.128025, 2021.
647 Goldberg, D. L., Vinciguerra, T. P., Anderson, D. C., Hembeck, L., Canty, T. P., Ehrman, S. H., Martins, D.
648 K., Stauffer, R. M., Thompson, A. M., Salawitch, R. J., and Dickerson, R. R.: CAMx ozone source
649 attribution in the eastern United States using guidance from observations during DISCOVER - AQ
650 Maryland, Geophys. Res. Lett., 43, 2249-2258, https://doi.org/10.1002/2015gl067332, 2016.
651 Goldstein, A. H., and Galbally, I. E.: Known and unexplored organic constituents in the earth's atmosphere,
652 Environ. Sci. Technol., 41, 1514-1521, https://doi.org/10.1021/es072476p, 2007.
653 Guan, Y., Wang, L., Wang, S., Zhang, Y., Xiao, J., Wang, X., Duan, E., and Hou, L. a.: Temporal variations
654 and source apportionment of volatile organic compounds at an urban site in Shijiazhuang, China, J.
655 Environ. Sci., 97, 25-34, https://doi.org/10.1016/j.jes.2020.04.022, 2020.
656 Guenther, A. B., Zimmerman, P. R., Harley, P. C., Monson, R. K., and Fall, R.: Isoprene and monoterpene
657 emission rate variability: Model evaluations and sensitivity analyses, J. Geophys. Res-Atmos., 98, 12609-
658 12617, https://doi.org/https://doi.org/10.1029/93JD00527, 1993.
659 Guo, H., Cheng, H. R., Ling, Z. H., Louie, P. K., and Ayoko, G. A.: Which emission sources are responsible
660 for the volatile organic compounds in the atmosphere of Pearl River Delta?, J. Hazard. Mater., 188, 116-
661 124, https://doi.org/10.1016/j.jhazmat.2011.01.081, 2011.
662 Guo, H., Ling, Z. H., Cheung, K., Wang, D. W., Simpson, I. J., and Blake, D. R.: Acetone in the atmosphere
663 of Hong Kong: Abundance, sources and photochemical precursors, Atmos. Environ., 65, 80-88,
664 https://doi.org/10.1016/j.atmosenv.2012.10.027, 2013.
665 Guo, J., Xu, Q., Yu, S., Zhao, B., and Zhang, M.: Investigation of atmospheric VOCs sources and ozone
666 formation sensitivity during epidemic closure and control: A case study of Zhengzhou, Atmos. Pollut.
667 Res., 15, https://doi.org/10.1016/j.apr.2023.102035, 2024.
668 He, Z., Li, G., Chen, J., Huang, Y., An, T., and Zhang, C.: Pollution characteristics and health risk assessment
669 of volatile organic compounds emitted from different plastic solid waste recycling workshops, Environ.
670 Int., 77, 85-94, https://doi.org/10.1016/j.envint.2015.01.004, 2015.
671 Hong, Z., Li, M., Wang, H., Xu, L., Hong, Y., Chen, J., Chen, J., Zhang, H., Zhang, Y., Wu, X., Hu, B., and
672 Li, M.: Characteristics of atmospheric volatile organic compounds (VOCs) at a mountainous forest site
673 and two urban sites in the southeast of China, Sci. Total. Environ., 657, 1491-1500,

https://doi.org/10.1016/j.scitotenv.2018.12.132, 2019.

Huang, B., Lei, C., Wei, C., and Zeng, G.: Chlorinated volatile organic compounds (Cl-VOCs) in environment — sources, potential human health impacts, and current remediation technologies, Environ. Int., 71, 118-138, https://doi.org/10.1016/j.envint.2014.06.013, 2014.

Huang, C., Shi, Y., Yang, M., Tong, L., Dai, X., Liu, F., Huang, C., Zheng, J., Li, J., and Xiao, H.: Spatiotemporal distribution, source apportionment and health risk assessment of atmospheric volatile organic compounds using passive air samplers in a typical coastal area, China, J. Clean. Prod., 423, 138741, https://doi.org/10.1016/j.jclepro.2023.138741, 2023.

Huang, J., Fung, J. C. H., Lau, A. K. H., and Qin, Y.: Numerical simulation and process analysis of typhoon-related ozone episodes in Hong Kong, J. Geophys. Res-Atmos., 110, https://doi.org/10.1029/2004jd004914, 2005.

Hui, L., Ma, T., Gao, Z., Gao, J., Wang, Z., Xue, L., Liu, H., and Liu, J.: Characteristics and sources of volatile organic compounds during high ozone episodes: A case study at a site in the eastern Guanzhong Plain, China, Chemosphere, 265, 129072, https://doi.org/10.1016/j.chemosphere.2020.129072, 2020.

Jorquera, H., and Rappenglück, B.: Receptor modeling of ambient VOC at Santiago, Chile, Atmos. Environ., 38, 4243-4263, https://doi.org/10.1016/j.atmosenv.2004.04.030, 2004.

Kim, E., and Hopke, P.: Comparison between conditional probability function and nonparametric regression for fine particle source directions, Atmos. Environ., 38, 4667–4673, https://doi.org/10.1016/j.atmosenv.2004.05.035, 2004.

Kleinman, L. I.: Ozone process insights from field experiments – part II: Observation-based analysis for ozone production, Atmos. Environ., 34, 2023-2033, https://doi.org/https://doi.org/10.1016/S1352-2310(99)00457-4, 2000.

Lerner, J. E. C., Sanchez, E. Y., Sambeth, J. E., and Porta, A. A.: Characterization and health risk assessment of VOCs in occupational environments in Buenos Aires, Argentina, Atmos. Environ., 55, 440-447, https://doi.org/10.1016/j.atmosenv.2012.03.041, 2012.

Li, J., Zhai, C., Yu, J., Liu, R., Li, Y., Zeng, L., and Xie, S.: Spatiotemporal variations of ambient volatile organic compounds and their sources in Chongqing, a mountainous megacity in China, Sci. Total. Environ., 627, 1442-1452, https://doi.org/10.1016/j.scitotenv.2018.02.010, 2018.

Li, Y., Wu, Z., Ji, Y., Chen, T., Li, H., Gao, R., Xue, L., Wang, Y., Zhao, Y., and Yang, X.: Comparison of the ozone formation mechanisms and VOCs apportionment in different ozone pollution episodes in urban Beijing in 2019 and 2020: Insights for ozone pollution control strategies, Sci. Total. Environ., 908,

https://doi.org/10.1016/j.scitotenv.2023.168332, 2024.

Li, Y., Yin, S., Yu, S., Yuan, M., Dong, Z., Zhang, D., Yang, L., and Zhang, R.: Characteristics, source apportionment and health risks of ambient VOCs during high ozone period at an urban site in central plain, China, Chemosphere, 250, 126283, https://doi.org/10.1016/j.chemosphere.2020.126283, 2020.

Lin, C., Ho, T. C., Chu, H., Yang, H., Chandru, S., Krishnarajanagar, N., Chiou, P., and Hopper, J. R.: Sensitivity analysis of ground-level ozone concentration to emission changes in two urban regions of southeast Texas, J. Environ. Manage., 75, 315-323, https://doi.org/10.1016/j.jenvman.2004.09.012, 2005.

Ling, Z. H., Guo, H., Cheng, H. R., and Yu, Y. F.: Sources of ambient volatile organic compounds and their contributions to photochemical ozone formation at a site in the Pearl River Delta, southern China, Environ. Pollut., 159, 2310-2319, https://doi.org/10.1016/j.envpol.2011.05.001, 2011.

Ling, Z. H., Guo, H., Zheng, J. Y., Louie, P. K. K., Cheng, H. R., Jiang, F., Cheung, K., Wong, L. C., and Feng, X. Q.: Establishing a conceptual model for photochemical ozone pollution in subtropical Hong Kong, Atmos. Environ., 76, 208-220, https://doi.org/10.1016/j.atmosenv.2012.09.051, 2013.

Liu, B., Liang, D., Yang, J., Dai, Q., Bi, X., Feng, Y., Yuan, J., Xiao, Z., Zhang, Y., and Xu, H.: Characterization and source apportionment of volatile organic compounds based on 1-year of observational data in Tianjin, China, Environ. Pollut., 218, 757-769, https://doi.org/10.1016/j.envpol.2016.07.072, 2016.

Liu, B., Yang, Y., Yang, T., Dai, Q., Zhang, Y., Feng, Y., and Hopke, P. K.: Effect of photochemical losses of ambient volatile organic compounds on their source apportionment, Environ. Int., 172, 107766, https://doi.org/10.1016/j.envint.2023.107766, 2023a.

Liu, T., Hong, Y., Li, M., Xu, L., Chen, J., Bian, Y., Yang, C., Dan, Y., Zhang, Y., Xue, L., Zhao, M., Huang, Z., and Wang, H.: Atmospheric oxidation capacity and ozone pollution mechanism in a coastal city of southeastern China: analysis of a typical photochemical episode by an observation-based model, Atmos. Chem. Phys., 22, 2173-2190, https://doi.org/10.5194/acp-22-2173-2022, 2022.

Liu, Y., Shao, M., Fu, L., Lu, S., Zeng, L., and Tang, D.: Source profiles of volatile organic compounds (VOCs) measured in China: Part I, Atmos. Environ., 42, 6247-6260, https://doi.org/10.1016/j.atmosenv.2008.01.070, 2008.

Liu, Y., Song, M., Liu, X., Zhang, Y., Hui, L., Kong, L., Zhang, Y., Zhang, C., Qu, Y., An, J., Ma, D., Tan, Q., and Feng, M.: Characterization and sources of volatile organic compounds (VOCs) and their related changes during ozone pollution days in 2016 in Beijing, China, Environ. Pollut., 257, 113599, https://doi.org/10.1016/j.envpol.2019.113599, 2020.

Liu, Y., Kong, L., Liu, X., Zhang, Y., Li, C., Zhang, Y., Zhang, C., Qu, Y., An, J., Ma, D., Tan, Q., Feng, M.,

and Zha, S.: Characteristics, secondary transformation, and health risk assessment of ambient volatile organic compounds (VOCs) in urban Beijing, China, Atmos. Pollut. Res., 12, 33-46, https://doi.org/10.1016/j.apr.2021.01.013, 2021.

Liu, Z., Hu, K., Zhang, K., Zhu, S., Wang, M., and Li, L.: VOCs sources and roles in O_3 formation in the central Yangtze River Delta region of China, Atmos. Environ., 302, 119755, https://doi.org/10.1016/j.atmosenv.2023.119755, 2023b.

Liu, Z., Wang, B., Wang, C., Sun, Y., Zhu, C., Sun, L., Yang, N., Fan, G., Sun, X., Xia, Z., Pan, G., Zhu, C., Gai, Y., Wang, X., Xiao, Y., Yan, G., and Xu, C.: Characterization of photochemical losses of volatile organic compounds and their implications for ozone formation potential and source apportionment during summer in suburban Jinan, China, Environ. Res., 238, 117158, https://doi.org/10.1016/j.envres.2023.117158, 2023c.

Lu, B., Zhang, Z., Jiang, J., Meng, X., Liu, C., Herrmann, H., Chen, J., Xue, L., and Li, X.: Unraveling the O_3-NO_x-VOCs relationships induced by anomalous ozone in industrial regions during COVID-19 in Shanghai, Atmos. Environ., 308, 119864, https://doi.org/10.1016/j.atmosenv.2023.119864, 2023.

Lyu, X. P., Chen, N., Guo, H., Zhang, W. H., Wang, N., Wang, Y., and Liu, M.: Ambient volatile organic compounds and their effect on ozone production in Wuhan, central China, Sci. Total. Environ., 541, 200-209, https://doi.org/10.1016/j.scitotenv.2015.09.093, 2016.

Meng, X., Jiang, J., Chen, T., Zhang, Z., Lu, B., Liu, C., Xue, L., Chen, J., Herrmann, H., and Li, X.: Chemical drivers of ozone change in extreme temperatures in eastern China, Sci. Total. Environ., 874, https://doi.org/10.1016/j.scitotenv.2023.162424, 2023.

Meng, Y., Song, J., Zeng, L., Zhang, Y., Zhao, Y., Liu, X., Guo, H., Zhong, L., Ou, Y., Zhou, Y., Zhang, T., Yue, D., and Lai, S.: Ambient volatile organic compounds at a receptor site in the Pearl River Delta region: Variations, source apportionment and effects on ozone formation, J. Environ. Sci., 111, 104-117, https://doi.org/10.1016/j.jes.2021.02.024, 2022.

Miller, L., Xu, X., Grgicak-Mannion, A., Brook, J., and Wheeler, A.: Multi-season, multi-year concentrations and correlations amongst the BTEX group of VOCs in an urbanized industrial city, Atmos. Environ., 61, 305-315, https://doi.org/10.1016/j.atmosenv.2012.07.041, 2012.

Min, R., Wang, F., Wang, Y., Song, G., Zheng, H., Zhang, H., Ru, X., and Song, H.: Contribution of local and surrounding area anthropogenic emissions to a high ozone episode in Zhengzhou, China, Environ. Res., 212, 113440, https://doi.org/10.1016/j.envres.2022.113440, 2022.

Ministry of Environmental Protection of China, 2012. Ambient air quality standards. (GB 3095-2012).

https://www.mee.gov.cn/ywgz/fgbz/bz/bzwb/dqhjbh/dqhjzlbz/201203/W020120410330232398521.pdf.

Ming, W., Wentai, C., Lin, Z., Wei, Q., Yong, Z., Xiangzhi, Z., and Xin, X.: Ozone pollution characteristics and sensitivity analysis using an observation-based model in Nanjing, Yangtze River Delta Region of China, J. Environ. Sci., https://doi.org/10.1016/j.jes.2020.02.027, 2020.

Mo, Z., Shao, M., Lu, S., Qu, H., Zhou, M., Sun, J., and Gou, B.: Process-specific emission characteristics of volatile organic compounds (VOCs) from petrochemical facilities in the Yangtze River Delta, China, Sci. Total. Environ., 533, 422-431, https://doi.org/10.1016/j.scitotenv.2015.06.089, 2015.

Monod, A., Sive, B. C., Avino, P., Chen, T., Blake, D. R., and Sherwood Rowland, F.: Monoaromatic compounds in ambient air of various cities: a focus on correlations between the xylenes and ethylbenzene, Atmos. Environ., 35, 135-149, https://doi.org/https://doi.org/10.1016/S1352-2310(00)00274-0, 2001.

Mozaffar, A., Zhang, Y., Fan, M., Cao, F., and Lin, Y.: Characteristics of summertime ambient VOCs and their contributions to O_3 and SOA formation in a suburban area of Nanjing, China, Atmos. Res., 240, 104923, https://doi.org/10.1016/j.atmosres.2020.104923, 2020.

Mozaffar, A., Zhang, Y., Lin, Y., Xie, F., Fan, M., and Cao, F.: Measurement report: High contributions of halocarbon and aromatic compounds to atmospheric volatile organic compounds in an industrial area, Atmos. Chem. Phys., 21, 18087-18099, https://doi.org/10.5194/acp-21-18087-2021, 2021.

MPS (The Ministry of Public Security of the People's Republic of China), 2022. The number of motor vehicles in China exceeded 400 million. https://www.mps.gov.cn/n2254314/n6409334/c8451247/content.html. (Accessed 10 October 2023).

Na, K., Kim, Y. P., Moon, K.-C., Moon, I., and Fung, K.: Concentrations of volatile organic compounds in an industrial area of Korea, Atmos. Environ., 35, 2747-2756, https://doi.org/https://doi.org/10.1016/S1352-2310(00)00313-7, 2001.

Nelson, B. S., Stewart, G. J., Drysdale, W. S., Newland, M. J., Vaughan, A. R., Dunmore, R. E., Edwards, P. M., Lewis, A. C., Hamilton, J. F., and Acton, W. J.: In situ ozone production is highly sensitive to volatile organic compounds in Delhi, India, Copernicus Publications, 17, https://doi.org/10.5194/ACP-21-13609-2021, 2021.

Nopmongcol, U., Koo, B., Tai, E., Jung, J., Piyachaturawat, P., Emery, C., Yarwood, G., Pirovano, G., Mitsakou, C., and Kallos, G.: Modeling Europe with CAMx for the Air Quality Model Evaluation International Initiative (AQMEII), Atmos. Environ., 53, 177-185, https://doi.org/https://doi.org/10.1016/j.atmosenv.2011.11.023, 2012.

Norris, G., Duvall, R., Brown, S., and Bai, S.: EPA Positive Matrix Factorization (PMF) 5.0. Fundamentals

and User Guide Prepared for the U.S. Environmental Protection Agency Office of Research and Development, Washington, DC (EPA/600/R-14/108; STI-9105115594-UG, April), 2014.

Pacifico, F., Harrison, S. P., Jones, C. D., and Sitch, S.: Isoprene emissions and climate, Atmos. Environ., 43, 6121-6135, https://doi.org/10.1016/j.atmosenv.2009.09.002, 2009.

Paulot, F., Crounse, J. D., Kjaergaard, H. G., Kürten, A., St Clair, J. M., Seinfeld, J. H., and Wennberg, P. O.: Unexpected Epoxide Formation in the Gas-Phase Photooxidation of Isoprene, Science, 325, 730-733, https://doi.org/10.1126/science.1172910, 2009.

Prendez, M., Carvajal, V., Corada, K., Morales, J., Alarcon, F., and Peralta, H.: Biogenic volatile organic compounds from the urban forest of the Metropolitan Region, Chile, Environ. Pollut., 183, 143-150, https://doi.org/10.1016/j.envpol.2013.04.003, 2013.

Qin, J., Wang, X., Yang, Y., Qin, Y., Shi, S., Xu, P., Chen, R., Zhou, X., Tan, J., and Wang, X.: Source apportionment of VOCs in a typical medium-sized city in North China Plain and implications on control policy, J. Environ. Sci., 107, 26-37, https://doi.org/10.1016/j.jes.2020.10.005, 2021.

Qin, Z., Xu, B., Zheng, Z., Li, L., Zhang, G., Li, S., Geng, C., Bai, Z., and Yang, W.: Integrating ambient carbonyl compounds provides insight into the constrained ozone formation chemistry in Zibo city of the North China Plain, Environ. Pollut., 324, https://doi.org/10.1016/j.envpol.2023.121294, 2023.

Ring, A. M., Canty, T. P., Anderson, D. C., Vinciguerra, T. P., He, H., Goldberg, D. L., Ehrman, S. H., Dickerson, R. R., and Salawitch, R. J.: Evaluating commercial marine emissions and their role in air quality policy using observations and the CMAQ model, Atmos. Environ., 173, 96-107, https://doi.org/10.1016/j.atmosenv.2017.10.037, 2018.

Seila, R. L., Main, H. H., Arriaga, J. L., Martínez V, G., and Ramadan, A. B.: Atmospheric volatile organic compound measurements during the 1996 Paso del Norte Ozone Study, Sci. Total. Environ., 276, 153-169, https://doi.org/https://doi.org/10.1016/S0048-9697(01)00777-X, 2001.

Sha, Q., Zhu, M., Huang, H., Wang, Y., Huang, Z., Zhang, X., Tang, M., Lu, M., Chen, C., Shi, B., Chen, Z., Wu, L., Zhong, Z., Li, C., Xu, Y., Yu, F., Jia, G., Liao, S., Cui, X., Liu, J., and Zheng, J.: A newly integrated dataset of volatile organic compounds (VOCs) source profiles and implications for the future development of VOCs profiles in China, Sci. Total. Environ., 793, 148348, https://doi.org/10.1016/j.scitotenv.2021.148348, 2021.

Shao, M., Zhang, Y., Zeng, L., Tang, X., Zhang, J., Zhong, L., and Wang, B.: Ground-level ozone in the Pearl River Delta and the roles of VOC and NO(x) in its production, J. Environ. Manage., 90, 512-518, https://doi.org/10.1016/j.jenvman.2007.12.008, 2009.

Shao, P., An, J., Xin, J., Wu, F., Wang, J., Ji, D., and Wang, Y.: Source apportionment of VOCs and the contribution to photochemical ozone formation during summer in the typical industrial area in the Yangtze River Delta, China, Atmos. Res., 176-177, 64-74, https://doi.org/10.1016/j.atmosres.2016.02.015, 2016.

Sharkey, T. D., Singsaas, E. L., Vanderveer, P. J., and Geron, C.: Field measurements of isoprene emission from trees in response to temperature and light, Tree. Physiol., 16, 649-654, https://doi.org/10.1093/treephys/16.7.649, 1996.

Sicard, P., De Marco, A., Agathokleous, E., Feng, Z., Xu, X., Paoletti, E., Rodriguez, J. J. D., and Calatayud, V.: Amplified ozone pollution in cities during the COVID-19 lockdown, Sci. Total. Environ., 735, 139542, https://doi.org/10.1016/j.scitotenv.2020.139542, 2020.

Sillman, S.: The relation between ozone, NO_x and hydrocarbons in urban and polluted rural environments, Atmos. Environ., 33, 1821–1845, https://doi.org/https://doi.org/10.1016/S1352-2310(98)00345-8, 1999.

Song, Y., Shao, M., Liu, Y., Lu, S., Kuster, W., Goldan, P., and Xie, S.: Source apportionment of ambient volatile organic compounds in Beijing, Environ. Sci. Technol., 41, 4348-4353, 2007.

Tang, J. H., Chan, L. Y., Chan, C. Y., Li, Y. S., Chang, C. C., Liu, S. C., Wu, D., and Li, Y. D.: Characteristics and diurnal variations of NMHCs at urban, suburban, and rural sites in the Pearl River Delta and a remote site in South China, Atmos. Environ., 41, 8620-8632, https://doi.org/10.1016/j.atmosenv.2007.07.029, 2007.

Thijsse, T. R., Oss, R. F. V., and Lenschow, P.: Determination of Source Contributions to Ambient Volatile Organic Compound Concentrations in Berlin, J. Air. Waste. Manage., 49, 1394-1404, https://doi.org/10.1080/10473289.1999.10463974, 1999.

Tsai, W. Y., Chan, L. Y., Blake, D. R., and Chu, K. W.: Vehicular fuel composition and atmospheric emissions in South China: Hong Kong, Macau, Guangzhou, and Zhuhai, Atmos. Chem. Phys., 6, 3281-3288, https://doi.org/10.5194/acp-6-3281-2006, 2006.

Uria-Tellaetxe, I., and Carslaw, D. C.: Conditional bivariate probability function for source identification, Environ. Modell. Softw., 59, 1-9, https://doi.org/10.1016/j.envsoft.2014.05.002, 2014.

Positive Matrix Factorization Model for environmental data analyses: https://www.epa.gov/airr-esearch/positive-matrix-factorization-modelenvironmentaldata-analyses, access: June, 2014.

Wang, B., Liu, Z., Li, Z., Sun, Y., Wang, C., Zhu, C., Sun, L., Yang, N., Bai, G., Fan, G., Sun, X., Xia, Z., Pan, G., Xu, C., and Yan, G.: Characteristics, chemical transformation and source apportionment of volatile organic compounds (VOCs) during wintertime at a suburban site in a provincial capital city, east China, Atmos. Environ., 298, 119621, https://doi.org/10.1016/j.atmosenv.2023.119621, 2023a.

Wang, M., Sheng, H., Liu, Y., Wang, G., Huang, H., Fan, L., and Ye, D.: Research on the diurnal variation characteristics of ozone formation sensitivity and the impact of ozone pollution control measures in "2 + 26" cities of Henan Province in summer, Sci. Total. Environ., 888, 164121, https://doi.org/10.1016/j.scitotenv.2023.164121, 2023b.

Wang, P., Chen, Y., Hu, J., Zhang, H., and Ying, Q.: Source apportionment of summertime ozone in China using a source-oriented chemical transport model, Atmos. Environ., 211, 79-90, https://doi.org/10.1016/j.atmosenv.2019.05.006, 2019.

Wang, X., Yin, S., Zhang, R., Yuan, M., and Ying, Q.: Assessment of summertime O_3 formation and the O_3-NO_x-VOC sensitivity in Zhengzhou, China using an observation-based model, Sci. Total. Environ., 813, 152449, https://doi.org/10.1016/j.scitotenv.2021.152449, 2022.

Wang, Y., Guo, H., Zou, S., Lyu, X., Ling, Z., Cheng, H., and Zeren, Y.: Surface O3 photochemistry over the South China Sea: Application of a near-explicit chemical mechanism box model, Environ. Pollut., 234, 155-166, https://doi.org/10.1016/j.envpol.2017.11.001, 2018.

Wang, Y., Wang, H., Guo, H., Lyu, X., Cheng, H., Ling, Z., Louie, P. K. K., Simpson, I. J., Meinardi, S., and Blake, D. R.: Long-term O_3–precursor relationships in Hong Kong: field observation and model simulation, Atmos. Chem. Phys., 17, 10919-10935, https://doi.org/10.5194/acp-17-10919-2017, 2017.

Watson, J. G., Chow, J. C., and Fujita, E. M.: Review of volatile organic compound source apportionment by chemical mass balance, Atmos. Environ., 35, 1567-1584, https://doi.org/10.1016/S1352-2310(00)00461-1, 2001.

Wu, R., Li, J., Hao, Y., Li, Y., Zeng, L., and Xie, S.: Evolution process and sources of ambient volatile organic compounds during a severe haze event in Beijing, China, Sci. Total. Environ., 560-561, 62-72, https://doi.org/10.1016/j.scitotenv.2016.04.030, 2016.

Wu, Y., Fan, X., Liu, Y., Zhang, J., Wang, H., Sun, L., Fang, T., Mao, H., Hu, J., Wu, L., Peng, J., and Wang, S.: Source apportionment of VOCs based on photochemical loss in summer at a suburban site in Beijing, Atmos. Environ., 293, https://doi.org/10.1016/j.atmosenv.2022.119459, 2023.

Wu, Y., Liu, B., Meng, H., Dai, Q., Shi, L., Song, S., Feng, Y., and Hopke, P. K.: Changes in source apportioned VOCs during high O_3 periods using initial VOC-concentration-dispersion normalized PMF, Sci. Total. Environ., 896, https://doi.org/10.1016/j.scitotenv.2023.165182, 2023.

Xia, L., Cai, C., Zhu, B., An, J., Li, Y., and Li, Y.: Source apportionment of VOCs in a suburb of Nanjing, China, in autumn and winter, J. Atmos. Chem., 71, 175-193, https://doi.org/10.1007/s10874-014-9289-6, 2014.

Xie, Y., and Berkowitz, C. M.: The use of positive matrix factorization with conditional probability functions in air quality studies: An application to hydrocarbon emissions in Houston, Texas, Atmos. Environ., 40, 3070-3091, https://doi.org/10.1016/j.atmosenv.2005.12.065, 2006.

Xie, Y., Cheng, C., Wang, Z., Wang, K., Wang, Y., Zhang, X., Li, X., Ren, L., Liu, M., and Li, M.: Exploration of O_3-precursor relationship and observation-oriented O_3 control strategies in a non-provincial capital city, southwestern China, Sci. Total. Environ., 800, 149422, https://doi.org/10.1016/j.scitotenv.2021.149422, 2021.

Xu, Z., Zou, Q., Jin, L., Shen, Y., Shen, J., Xu, B., Qu, F., Zhang, F., Xu, J., Pei, X., Xie, G., Kuang, B., Huang, X., Tian, X., and Wang, Z.: Characteristics and sources of ambient Volatile Organic Compounds (VOCs) at a regional background site, YRD region, China: Significant influence of solvent evaporation during hot months, Sci. Total. Environ., 857, 159674, https://doi.org/10.1016/j.scitotenv.2022.159674, 2023.

Yan, D., Zhang, Z., Jin, Z., Li, M., Sheridan, S. C., and Wang, T.: Ozone variability driven by the synoptic patterns over China during 2014–2022 and its implications for crop yield and economy, Atmos. Pollut. Res., 14, 101843, https://doi.org/10.1016/j.apr.2023.101843, 2023.

Yang, L., Yuan, Z., Luo, H., Wang, Y., Xu, Y., Duan, Y., and Fu, Q.: Identification of long-term evolution of ozone sensitivity to precursors based on two-dimensional mutual verification, Sci. Total. Environ., 760, 143401, https://doi.org/10.1016/j.scitotenv.2020.143401, 2021.

Yu, S., Su, F., Yin, S., Wang, S., Xu, R., He, B., Fan, X., Yuan, M., and Zhang, R.: Characterization of ambient volatile organic compounds, source apportionment, and the ozone-NO_x-VOC sensitivities in a heavily polluted megacity of central China: effect of sporting events and emission reductions, Atmos. Chem. Phys., 21, 15239-15257, https://doi.org/10.5194/acp-21-15239-2021, 2021.

Yu, S., Wang, S., Xu, R., Zhang, D., Zhang, M., Su, F., Lu, X., Li, X., Zhang, R., and Wang, L.: Measurement report: Intra- and interannual variability and source apportionment of volatile organic compounds during 2018–2020 in Zhengzhou, central China, Atmos. Chem. Phys., 22, 14859-14878, https://doi.org/10.5194/acp-22-14859-2022, 2022.

Yuan, B., Shao, M., de Gouw, J., Parrish, D. D., Lu, S., Wang, M., Zeng, L., Zhang, Q., Song, Y., Zhang, J., and Hu, M.: Volatile organic compounds (VOCs) in urban air: How chemistry affects the interpretation of positive matrix factorization (PMF) analysis, J. Geophys. Res-Atmos., 117, 24302, https://doi.org/10.1029/2012jd018236, 2012.

Yuan, Z., Zhong, L., Lau, A. K. H., Yu, J. Z., and Louie, P. K. K.: Volatile organic compounds in the Pearl River Delta: Identification of source regions and recommendations for emission-oriented monitoring

strategies, Atmos. Environ., 76, 162-172, https://doi.org/10.1016/j.atmosenv.2012.11.034, 2013.

Yurdakul, S., Civan, M., Kuntasal, Ö., Doğan, G., Pekey, H., and Tuncel, G.: Temporal variations of VOC concentrations in Bursa atmosphere, Atmos. Pollut. Res., 9, 189-206, https://doi.org/10.1016/j.apr.2017.09.004, 2018.

Zeng, X., Han, M., Ren, G., Liu, G., Wang, X., Du, K., Zhang, X., and Lin, H.: A comprehensive investigation on source apportionment and multi-directional regional transport of volatile organic compounds and ozone in urban Zhengzhou, Chemosphere, 334, 139001, https://doi.org/10.1016/j.chemosphere.2023.139001, 2023.

Zhang, D., He, B., Yuan, M., Yu, S., Yin, S., and Zhang, R.: Characteristics, sources and health risks assessment of VOCs in Zhengzhou, China during haze pollution season, J. Environ. Sci., 108, 44-57, https://doi.org/10.1016/j.jes.2021.01.035, 2021.

Zhang, H., Wang, Y., Hu, J., Ying, Q., and Hu, X. M.: Relationships between meteorological parameters and criteria air pollutants in three megacities in China, Environ. Res., 140, 242-254, https://doi.org/10.1016/j.envres.2015.04.004, 2015.

Zhang, L., Li, H., Wu, Z., Zhang, W., Liu, K., Cheng, X., Zhang, Y., Li, B., and Chen, Y.: Characteristics of atmospheric volatile organic compounds in urban area of Beijing: Variations, photochemical reactivity and source apportionment, J. Environ. Sci., 95, 190-200, https://doi.org/10.1016/j.jes.2020.03.023, 2020.

Zhang, Y., Li, R., Fu, H., Zhou, D., and Chen, J.: Observation and analysis of atmospheric volatile organic compounds in a typical petrochemical area in Yangtze River Delta, China, J. Environ. Sci., 71, 233-248, https://doi.org/10.1016/j.jes.2018.05.027, 2018.

Zhang, Y. H., Su, H., Zhong, L. J., Cheng, Y. F., Zeng, L. M., Wang, X. S., Xiang, Y. R., Wang, J. L., Gao, D. F., and Shao, M.: Regional ozone pollution and observation-based approach for analyzing ozone–precursor relationship during the PRIDE-PRD2004 campaign, Atmos. Environ., 42, 6203-6218, https://doi.org/10.1016/j.atmosenv.2008.05.002, 2008.

Zhang, Z., Zhang, Y., Wang, X., Lü, S., Huang, Z., Huang, X., Yang, W., Wang, Y., and Zhang, Q.: Spatiotemporal patterns and source implications of aromatic hydrocarbons at six rural sites across China's developed coastal regions, J. Geophys. Res-Atmos., 121, 6669-6687, https://doi.org/10.1002/2016jd025115, 2016.

Zhang, Z., Sun, Y., and Li, J.: Characteristics and sources of VOCs in a coastal city in eastern China and the implications in secondary organic aerosol and O_3 formation, Sci. Total. Environ., 887, 164117, https://doi.org/10.1016/j.scitotenv.2023.164117, 2023.

Zhao, C., Sun, Y., Zhong, Y., Xu, S., Liang, Y., Liu, S., He, X., Zhu, J., Shibamoto, T., and He, M.: Spatio-temporal analysis of urban air pollutants throughout China during 2014-2019, Air. Qual. Atmos. Hlth., 14, 1619-1632, https://doi.org/10.1007/s11869-021-01043-5, 2021.

Zhao, Y., Chen, L., Li, K., Han, L., Zhang, X., Wu, X., Gao, X., Azzi, M., and Cen, K.: Atmospheric ozone chemistry and control strategies in Hangzhou, China: Application of a 0-D box model, Atmos. Res., 246, https://doi.org/10.1016/j.atmosres.2020.105109, 2020.

Zhu, B., Huang, X., Xia, S., Lin, L., Cheng, Y., and He, L.: Biomass-burning emissions could significantly enhance the atmospheric oxidizing capacity in continental air pollution, Environ. Pollut., 285, 117523, https://doi.org/10.1016/j.envpol.2021.117523, 2021.

Zong, R., Yang, X., Wen, L., Xu, C., Zhu, Y., Chen, T., Yao, L., Wang, L., Zhang, J., Yang, L., Wang, X., Shao, M., Zhu, T., Xue, L., and Wang, W.: Strong ozone production at a rural site in theNorth China Plain: Mixed effects of urban plumesand biogenic emissions, J. Environ. Sci., 71, 261-270, https://doi.org/10.1016/j.jes.2018.05.003, 2018.

Zou, Y., Yan, X. L., Flores, R. M., Zhang, L. Y., Yang, S. P., Fan, L. Y., Deng, T., Deng, X. J., and Ye, D. Q.: Source apportionment and ozone formation mechanism of VOCs considering photochemical loss in Guangzhou, China, Sci. Total. Environ., 903, 166191, https://doi.org/10.1016/j.scitotenv.2023.166191, 2023.